

GORAM: Graph-oriented ORAM for Efficient Ego-centric Queries on Federated Graphs

Xiaoyu Fan
Tsinghua University
fxy23@mails.tsinghua.edu.cn

Kun Chen
Ant Group
ck413941@antgroup.com

Jiping Yu
Tsinghua University
yjp19@mails.tsinghua.edu.cn

Xiaowei Zhu
Ant Group
robert.zxw@antgroup.com

Yunyi Chen
Tsinghua University
cyy23@mails.tsinghua.edu.cn

Huanchen Zhang
Tsinghua University
huanchen@tsinghua.edu.cn

Wei Xu
Tsinghua University
weixu@tsinghua.edu.cn

Abstract

Ego-centric queries, focusing on a target vertex and its direct neighbors, are essential for various applications. Enabling such queries on graphs owned by mutually distrustful data providers without breaching privacy holds promise for more comprehensive results.

In this paper, we propose GORAM, a graph-oriented data structure that enables efficient ego-centric queries on federated graphs with strong privacy guarantees. GORAM leverages *secure multi-party computation (MPC)* and ensures that no information about the graphs or the querying keys is exposed during the process. For practical performance, GORAM partitions the federated graph and constructs an *Oblivious RAM (ORAM)*-inspired index atop these partitions. This design enables each ego-centric query to process only a single partition, which can be accessed fast and securely.

Utilizing GORAM, we develop a prototype querying engine on a real-world MPC framework. We then conduct a comprehensive evaluation using five commonly used queries similar to the LinkBench workload description [11] on both synthetic and real-world graphs. Our evaluation shows that all five queries can be completed in just 58.1 milliseconds to 35.7 seconds, even on graphs with up to 41.6 million vertices and 1.4 billion edges. To the best of our knowledge, this represents the first instance of processing billion-scale graphs with practical performance on MPC.

PVLDB Reference Format:

Xiaoyu Fan, Kun Chen, Jiping Yu, Xiaowei Zhu, Yunyi Chen, Huanchen Zhang, and Wei Xu. GORAM: Graph-oriented ORAM for Efficient Ego-centric Queries on Federated Graphs. PVLDB, 18(1): XXX-XXX, 2025. doi:XX.XX/XXX.XX

PVLDB Artifact Availability:

The source code, data, and/or other artifacts have been made available at <https://github.com/Fannxy/GORAM-ABY3>.

This work is licensed under the Creative Commons BY-NC-ND 4.0 International License. Visit <https://creativecommons.org/licenses/by-nc-nd/4.0/> to view a copy of this license. For any use beyond those covered by this license, obtain permission by emailing info@vldb.org. Copyright is held by the owner/author(s). Publication rights licensed to the VLDB Endowment.

Proceedings of the VLDB Endowment, Vol. 18, No. 1 ISSN 2150-8097.
doi:XX.XX/XXX.XX

1 Introduction

Privacy-preserving federated query engines allow data providers to collaboratively compute the query result while keeping the input and all the intermediate results private. It becomes increasingly important with demands from many industries to share their data.

The purpose of this paper is to support federated queries on graphs, specifically the crucial *ego-centric* queries that target a specified vertex and all its direct neighbors. This basic type of queries has many applications, especially if multiple parties can cooperate. For example, by analyzing the relations among suspicious accounts, commercial banks can effectively detect money laundering from the transaction graphs [45, 53]. Quick identification of people exposed to an infected person is essential in a pandemic, and obviously the results become more thorough if we join data from multiple providers [41]. As LinkBench [11] reports, neighbor filtering on the given account, a typical ego-centric query, constitutes 55.6% of all queries at Meta. In fact, all queries in LinkBench are ego-centric.

The above motivating examples demonstrate that both the graph and the query keys contain sensitive information. Therefore, it is crucial to keep both of them private. While ego-centric queries are easy to do in plaintext, their efficiency highly depends on the graph-data-aware organizations, such as caches for popular vertices [19, 64]. However, this is in conflict with the privacy requirements in our federated setting. Unlike tabular data, where the schema is public and we only need to protect the data and query keys, the *graph structure* information also needs to be protected. E.g., whether a particular vertex or edge exists, the degree of a certain vertex, and even the distribution of the vertex degrees are all considered private information. For example, disclosing an edge in the transaction graph could expose sensitive relationships between accounts, thus necessitating protection.

One typical method to implement private queries on federated data is to use *secure multi-party computation (MPC)* [65] throughout the query process [12, 13, 17, 39, 58]. MPC is a cryptographic technique that allows multiple parties to jointly compute a function on their private inputs, guaranteeing that no information is leaked.

The straightforward idea for graph is to encode the entire adjacency matrix with MPC [16] and thus hide the entire graph, including the structure. Unfortunately, the representation requires

at least $O(|V|^2)$ space, where $|V|$ is the number of vertices. As real-world large graphs are sparse [26], this representation wastes a vast amount of memory to store non-existent edges (to protect the existence of edges), making it impractical for large graphs.

Nayak et al. [51] propose an innovative way to protect the graph structure by encoding and encrypting both the vertices and edges into an identical form and storing them in a *secure list*, thereby reducing the space overhead to $O(|V| + |E|)$, where $|E|$ is the number of edges. Given that $|V| + |E| \ll |V|^2$ for real-world graphs, the efficient space utilization makes this representation popular in secure graph processing [10, 37, 46, 47, 51]. However, to perform an ego-centric query while keeping the query key private, we need to scan the entire list, leading to $O(|V| + |E|)$ time complexity.

We observe that despite the space-inefficiency, using a well-studied cryptographic technique called *Oblivious RAM (ORAM)* [31, 66], which allows accessing the i th element of an array in sublinear time without revealing i , we can secretly access any element of an adjacency matrix sublinearly, providing sublinear query time. Our key idea is that if we can split the edge list into multiple partitions and build a matrix on top of the partitions, we can reduce the space size and only scan one partition for each query.

We propose GORAM, a graph-oriented data structure to support efficient ego-centric queries on large-scale federated graphs with strong privacy guarantees. In a nutshell, GORAM splits the vertices into multiple chunks and then segments the graph into a “matrix” of edge lists. We carefully plan the segmentation so that each edge list contains all edges starting from vertices in the row’s chunk and destinations in the column’s. In this way, the graph is organized as multiple *partitions*, satisfying that all the information needed for each ego-centric query is contained in *exactly* one partition. Logically, all partitions together contain the entire edge list of the graph, and the matrix serves as a secure *index* mapping a vertex or edge ID to a particular partition. Using GORAM, we can locate a particular partition sublinearly, and then we only need to scan the partition, greatly reducing running time (Section 4.2). While current ORAM only supports addressing into a single element, we extend the idea so that we can access a full partition efficiently and privately, maximizing benefits from vectorization and parallelism (Section 4.3). While GORAM is designed agnostic to underlying MPC protocols, we find that some widely used protocols, e.g., ABY3 [49], allow us to design a constant-round shuffling protocol, vastly accelerating ORAM initiation (Section 4.4). Based on GORAM, we can easily implement crucial queries. We implement five types of ego-centric queries, including *edge existence*, *1-hop neighbors*, *neighbors filtering*, etc., covering all the LinkBench queries [11] (Section 5).

We evaluate the above queries on three real-world and thirty synthetic graphs with varied distributions and sizes. Results in Section 7 show remarkable efficiency and scalability of GORAM. On the largest graph, Twitter [18], with more than 41.6 million vertices and 1.4 billion edges, all the queries can be finished within 35.7 seconds, and the fastest query only takes 58.1 milliseconds, showing 2 to 3 orders of magnitude speedup over the existing secure graph data structures. Also, the initialization of GORAM only requires less than 3.0 minutes. We provide a detailed performance analysis using the synthetic graphs and show that GORAM outperforms the existing data structures across varied distributions and sizes. To the best of our knowledge, GORAM is the first to support graphs

with more than one *billion* edges in secure computations, which is 2-orders-of-magnitude larger than the prior arts [10, 37, 47].

In summary, our contributions include:

(1) We propose GORAM, a graph-oriented data structure to support efficient sublinear ego-centric queries on federated graphs, guaranteeing strong privacy.

(2) We design comprehensive optimizations for practical performance on large-scale graphs, including local processing, lifecycle parallelisms, and a constant-round shuffling protocol.

(3) We develop a prototype secure querying engine based on GORAM and evaluate it comprehensively using five commonly used queries on 33 synthetic and real-world graphs, demonstrating remarkable efficiency and scalability.

2 Cryptography Background

2.1 Secure Multi-party Computation (MPC)

Secure Multi-party Computation (MPC) allows multiple distrusting parties to jointly compute a function while keeping each party’s input private. Note that the role of a “party” is to participate in the computation rather than protecting their private data.

Secret sharing is a popular technique in MPC [65]. A (t, n) -*secret sharing* schema splits sensitive data x to n parties, satisfying that any t parties can reconstruct x while fewer than t parties learn nothing about x . Similar to [10, 29, 39, 49], GORAM adopts the efficient $(2, 3)$ -secret sharing with *boolean* secret share. This scheme splits a number x into (x_1, x_2, x_3) with each x_i ($i \in \{1, 2, 3\}$) being uniformly random such that $x \equiv x_1 \oplus x_2 \oplus x_3$ (\oplus denotes bitwise XOR). Each party owns two shares: (x_1, x_2) , (x_2, x_3) , or (x_3, x_1) . Any particular party learns nothing about x , but any two parties can reconstruct x . Denote the boolean secret shares (x_1, x_2, x_3) as $\llbracket x \rrbracket$.

Secure operations. For a variety of operations (op) such as XOR, AND, OR, +, \times , and comparisons ($>$, \geq , $=$), we can use the MPC protocols (OP) to compute $z = \text{op}(x, y)$ collaboratively and securely: $\llbracket z \rrbracket = \text{OP}(\llbracket x \rrbracket, \llbracket y \rrbracket)$, where efficient arithmetic operations rely on transforming $\llbracket x \rrbracket$ into $\llbracket x \rrbracket^A$ such that $x \equiv x_1^A + x_2^A + x_3^A \pmod{2^k}$ [27, 49]. Except for XOR and +, other operations require at least one round of communication among the computation parties. It is common to batch the operations (similar to SIMD) to amortize the communication cost [39, 49].

Security guarantees. A well-designed MPC protocol can guarantee privacy and correctness against a specific *adversary model*. Common classifications include *semi-honest* vs. *malicious*, determined by whether the corrupted parties can deviate from the protocol and *honest*- vs. *dishonest*-majority, contingent on the corruption proportion. GORAM adopts all its MPC protocols from ABY3 [49] and Araki et al. [10], thus inheriting their semi-honest and honest-majority adversary model, same as [10, 29, 39, 49]. Note that GORAM is agnostic to the underlying protocols and can be adapted to others.

2.2 Oblivious RAM (ORAM)

Oblivious RAM (ORAM) [31] aims to implement oblivious *indexing*, i.e., accessing the i th element in an array while keeping i secret. ORAM offers two desirable properties: 1) it hides the access patterns, i.e., for *any* two indices i, j , servers performing the access cannot distinguish whether the index is i or j , protecting the privacy of the query keys; 2) it enables sub-linear-complexity

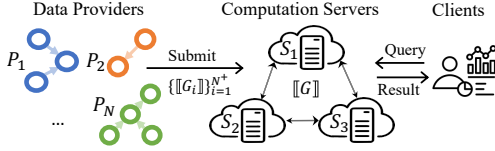


Figure 1: Logical Roles in Private Querying Process

accesses, thereby providing scalability. The original ORAM, e.g., Path ORAM [56], is designed for the *client-server* scenario, where a single client stores and retrieves her own private data on a single untrusted server [31]. In other words, ORAMs do not support the case where the underlying data comes from multiple data providers nor allow a third-party client (not the data provider) to access data. **Distributed ORAM (DORAM)** adds support to multiple data providers by using a group of computation servers that together hold the secret-shared data [44]. The servers can jointly access the target secret element given the secret-shared index, i.e., compute $[[arr[i]]] = [[arr]][[i]]$ without leaking the index. We build the index of GORAM by extending the classic Square-root ORAM [66]. Note that GORAM is agnostic to the specific DORAM implementations, and we choose Square-root ORAM because it has two desirable properties, in addition to simplicity: (1) it offers sublinear access time, and (2) it circumvents the reliance on any specific ciphers that may potentially degrade security. Section 8 provides discussion on other DORAM structures [20, 28, 29, 57, 66]. All the ORAM in the following denotes Square-root ORAM.

3 Overview

GORAM is a query engine designed to support private, ego-centric queries on federated graphs. There are three types of roles: (1) arbitrary number of *data providers*, each of which owns part of the graph that we call the *private graph*; (2) three *computation servers* that run the MPC protocol to process queries; and (3) an arbitrary number of *clients* who submit queries to the computation servers and receive the results. Similar to [39], the roles are decoupled. Each party can hold any combination of *different* roles, e.g., it can be both a data provider and a server. To be useful in the real world, we want GORAM to satisfy the following requirements:

- (1) *Functionality*: we want to support *arbitrary* ego-centric queries, allowing us to perform any filter or aggregation on a target vertex or edge along with all its direct neighbors.
- (2) *Privacy*: we want to keep two information private: (a) the query keys, i.e., the target vertices or edges; and (b) the graph, including the graph structure and the attributes of vertices and edges. Also, although the query result is revealed to the client, the client cannot infer which data provider contributed to the result.
- (3) *Scalability*: we want to support graphs with *billions* of edges, meeting the need for real-world graphs. Also, we anticipate responses within a few seconds on graphs with this scale.

3.1 Formalization

Private ego-centric queries on federated graphs. We assume a *global* directed graph $G = (V, E)$ is distributed among N data providers $P_i, i \in [N]$, $[N] = \{1, 2, \dots, N\}$. V and E denote the vertex and edge sets, respectively. Each edge $e \in E$ has a source and a destination vertex, v_s and v_d . We assume the edges (v_s, v_d) are different

because they may contain different attributes, e.g., timestamps [11]. We transform undirected graphs into directed ones by representing each edge with two directed edges.

Each *data provider* P_i owns a private graph $G_i = (V_i, E_i)$, satisfying that $V_i \subseteq V, E_i \subseteq E, E = \cup_{i \in [N]} E_i$ is the set of all edges, and it is always private. V is the set of all possible vertices, which is public. Because the complexity of GORAM is independent of $|V|$, we can safely set it to all the possible vertex names (e.g., a 64-bit ID), without leaking any information about the actual set of vertices. For *Mat* that does not support a large V , we set V as the union of all V_i 's and make it public. There are three semi-honest *computation servers* $S_i, i \in \{1, 2, 3\}$ holding the secret global graph $[[G]] = (V, [[E^+]])$ and carrying all the query processing, where $E^+ \supseteq E$ is a super-set of E because it may contain dummy edges for privacy. Each *client* can submit an ego-centric query with a secret key of either a vertex $[[v]]$ or edge $([[v_s]], [[v_d]])$ ($v, v_s, v_d \in V$) to the computation servers and receive the results. The ego-centric query can be an arbitrary filter or aggregation on the sub-graph $G_{\text{sub}} = (V_{\text{sub}}, E_{\text{sub}})$ containing all the direct neighbors of the target vertex v and the corresponding edges (v, v^*) if $(v, v^*) \in E$, or all edges $(v_s, v_d) \in E$. Ego-centric queries refer to both vertex- and edge-centric queries.

Threat model. We assume all roles *semi-honest*, and there exists an adversary who can compromise at most one computing server and see all of its internal states, similar to [10, 12, 29, 39]. Also, we assume the authentication of the data providers is conducted through the *ring signature* [52], a cryptographic technique enabling anonymous authentication.

3.2 Strawman Solutions

Two classic data structures are used to present the secure graph, i.e., *adjacency matrix* (*Mat*) [16] and *edge list* (*List*) [10, 46, 47, 51].

Based on Mat. With the public vertex set V , data providers can locally construct the $|V|^2$ adjacency matrix, encrypt it into secret-shared matrix and transfer the shares to the computation servers. Each server adds up the N secret matrices to form the secret matrix of the global graph G . Because *Mat* is a $|V| \times |V|$ matrix, we can naively adopt the ORAM for efficient access. Specifically, we build two ORAMs, *adj-VORAM*, operating over $|V|$ matrix rows (source vertices) and *adj-EORAM*, operating over an array of $|V|^2$ matrix elements (edges). For a vertex query on v_i , we access the $[[i]]$ th row from the *adj-VORAM*. This row contains $|V|$ elements, each representing the edge number between v_i and $v_j, j \in [|V|]$. For an edge query on (v_i, v_j) , we access the element $[[i * |V| + j]]$ from the *adj-EORAM*, which contains the number of edge (v_i, v_j) .

Mat is simple but never practical because of three issues. The most fatal one is the $O(|V|^2)$ space cost, making it impractical for real-world sparse graphs [6, 11, 26, 63]. Secondly, to limit V , we need to expose the actual vertex set, instead of just the possible namespace, public to all parties, leaking the information of the global set (e.g., the global customer list). Lastly, we cannot support multi-graph, i.e., edges with different attributes between a single pair of vertices, which is desirable in applications like transactions. **Based on List.** Each data provider P_i can simply create a secret-shared list of its edges $([[u]], [[v]])$, and optionally other attributes like timestamps. The compute servers can then concatenate the N secret lists to create the global edge list. In this way, the only

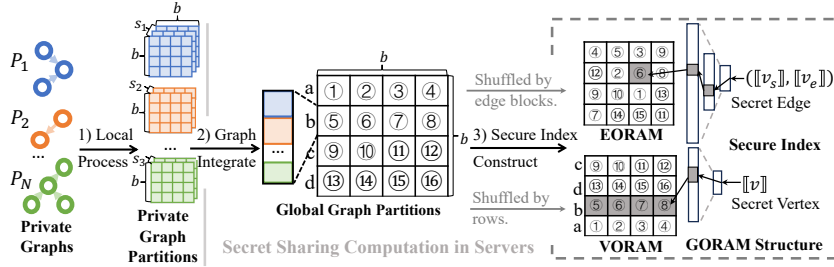


Figure 2: GORAM Initialization and Structure Overview

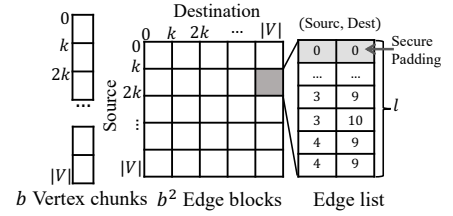


Figure 3: Graph Partition ($k = 2, |V| = 10$)

information leaked to the servers is the total number of edges from each provider. To protect these numbers, providers can append extra ϵ_i dummy edges, i.e., $([0], [0])$, before sending to the servers.

Although edge list is much more compact, the main issue with it is the access efficiency. Because all the edges are encrypted, and we have no knowledge about the existing vertices and edges, we can only scan the whole *List* for each ego-centric query, which introduces $O(|E|)$ complexity.

In summary, the two strawman solutions are either too costly on storage or on access time. A viable solution should allow a compact space while supporting sublinear access complexity.

3.3 GORAM Design

The high-level idea of GORAM is to split the graph into a “matrix” of edge lists. Intuitively, the matrix structure enables building ORAMs on top of the graph, circumventing the need for a full scan for each query. Simultaneously, the use of internal edge lists averts the $O(|V|^2)$ space complexity associated with the *Mat* structure. This approach seeks to achieve both space- and query-efficiency.

GORAM Overview. As Figure 2 shows, GORAM is a secret-shared data structure of the global graph $\llbracket G \rrbracket$, held by the computation servers. GORAM randomly shuffles the public vertex set V , splits it into b vertex chunks and then splits the graph $\llbracket G \rrbracket$ into a “matrix” of b^2 blocks, each block contains *all* the edges starting from and ending in two specific vertex chunks, and each row of the blocks correspondingly contains *all* the direct neighbors of a specific vertex chunk. This gives us two types of *partitions*: the block forms the partition for edge-centric queries, and the row of the blocks constitutes the partition for vertex-centric queries. GORAM then constructs $\llbracket G \rrbracket$ into VORAM and EORAM, which can securely access the partition given the secret vertex or edge. The indexing is achieved by modeling the partitions as ORAM, and we extend its functionality from accessing *array-of-elements* to *array-of-partitions*.

GORAM can be securely and efficiently initialized through three steps: (1) each data provider locally processes her private graph into secret-shared partitions; (2) the computation servers integrate all the partitions of private graphs into the global graph $\llbracket G \rrbracket$; and (3) the computation servers construct the secure indices for the partitions. The details of GORAM are illustrated in Section 4.

Through GORAM, we can implement arbitrary and efficient ego-centric queries easily. The clients can submit a provided query with a secret query key. For each query, the computation servers receive the query key, find the partition containing the key using GORAM, execute the query on the partition, and return the result to the client. We provide five query examples in Section 5.

Privacy guarantees. GORAM provides two guarantees: (1) *clients’ query key privacy*: no other party can learn anything about the client’s query key; (2) *data providers’ graph privacy*: no other party can learn any information about the data provider’s private graph, which includes the graph structure and the attributes of vertices and edges. Additionally, the client who receives the query result learns nothing except the result, including which provider contributes to it. Section 6.1 shows how GORAM ensures these guarantees.

4 Graph-Oriented ORAM (GORAM)

To satisfy the requirements in Section 3, GORAM splits the global graph G into a “matrix” of edge lists, forming a 2d-partitioned data structure, as Figure 3 shows. This structure groups every successive k vertices into a chunk according to randomly shuffled IDs from the range $\llbracket V \rrbracket = \{1, 2, \dots, |V|\}$, thereby creating $b = \lceil \frac{|V|}{k} \rceil$ chunks. Then, it splits the global graph into b^2 blocks of edge lists for each pair of chunks. Specifically, each block (s, d) contains all the edges $\{(v_s, v_d)\}$, with v_s and v_d belonging to the s th and d th chunk, respectively. To ensure security, each block is equalized in length with dummy edges, making the blocks indistinguishable.

It is worth noting that if an edge (v_s, v_d) exists, it is contained in a single edge block $(\lceil \frac{v_s}{k} \rceil, \lceil \frac{v_d}{k} \rceil)$. For each vertex v , all the direct outgoing neighbors¹ are included in the $\lceil \frac{v}{k} \rceil$ th row of b blocks. We heuristically choose a k based on the density of the graph because many real-world graphs like social graphs or transaction graphs have well-known character D [26]. Given that $D = \frac{|E|}{|V|}$ is the density of the graph, we use a default $k = \frac{|V|}{D}$, making the b independent of $|V|$. The block and row of blocks are the graph *partitions* for edge- and vertex-centric queries, respectively. Obviously, *only* one partition needs to be processed for each query. GORAM then builds the partitions as ORAMs to enable secure and fast access.

4.1 Preliminaries of Square-root ORAM

For readers unfamiliar with this area, we briefly introduce the Square-root ORAM [66], which GORAM extends for graph queries.

The key idea of Square-root ORAM is to shuffle an array (*arr*) according to a random permutation π , then build an index map on π that translates the secret logical index $\llbracket i \rrbracket$ to the plaintext physical index p in the shuffled data (\overline{arr}), where $\overline{arr}[i] \equiv \overline{arr}[p]$. Specifically, after shuffling $\overline{arr} = \pi(arr)$, ORAM explicitly stores the permutation representation $\tilde{\pi} = \pi^{-1}(L)$, $L = \{0, 1, \dots, n-1\}$ in

¹If the bi-directional neighbors are interested, the in-going neighbors are included in the $\lceil \frac{v}{k} \rceil$ th column of the 2d-partition.

secret shares, where n is size of arr and π^{-1} is the inverse permutation of π , i.e., $\pi^{-1}(\pi(arr)) \equiv arr$. Each $\tilde{\pi}[i]$ records the location of $arr[i]$ in \tilde{arr} . The index map of π is constructed as a recursive ORAM, where P successive elements of $\tilde{\pi}$ are packed as a single element and then build an ORAM for the $\frac{|\tilde{\pi}|}{P}$ elements recursively until the size is no greater than T . To access the j th element in arr (i.e., $arr[j]$), it is equivalent to access the $(\tilde{\pi}[j])$ th element in $\tilde{arr}[\tilde{\pi}[j]]$. Then we recur to the ORAMs built for $\tilde{\pi}$ to find $\tilde{\pi}[j]$.

Intuitively, each different logical index $[i]$ reveals a different random index, thereby keeping the access pattern private. To address the issue when repeating the same logical indices, Square-root ORAM employs a *stash* that stores the accessed element each time. For each logical index, we first try to find it in the stash. We only use this index to access the ORAM if it is *not* in the stash; otherwise, we pick an unused index to access the ORAM. Therefore, one always sees an access to stash and one to the ORAM and thus cannot distinguish whether the logical index is repeated. When the stash reaches capacity, we need to rebuild the ORAM. By default, the stash size is set to $T = \sqrt{n}$, where n is the number of elements in the ORAM. For read-only accesses, ORAMs can be continuously built in the background, allowing immediate replacement with a fresh ORAM when the stash is full. Disregarding the cost of rebuilding, the average access cost over T elements is $O(PT \log(\frac{n}{T}))$.

4.2 GORAM Initialization and Access

The GORAM initialization involves three steps:

Step 1 - Each data provider locally partition the private graph.

Because the global V is public, each data provider P_i can locally split the private graph G_i into the same b^2 blocks according to the public k . Each P_i initializes b^2 blocks using the global V regardless of the vertices actually owned in the private V_i . P_i then traverses the edge list E_i , pushing each edge (v_s, v_d) to block (s, d) , where $\lceil \frac{v_s}{k} \rceil = s$ and $\lceil \frac{v_d}{k} \rceil = d$, and sorting each block using the key $v_s || v_d$ (i.e., concatenation of the source and destination vertices).²

To protect the graph structure, it's crucial that each block is aligned to a uniform size \bar{l} . This public parameter is heuristically set to a default value of 8 to avoid excessive padding. The alignment includes two steps: (1) Each P_i pads blocks with dummy edges, i.e., $(0, 0)$, to align all blocks to the maximum block size l_i , thus protecting the edge distributions of each chunk; (2) If l_i is less than \bar{l} , P_i pads each block with $\bar{l} - l_i$ dummy edges. Otherwise, P_i divides the partitioned graph into $s_i = \lceil \frac{l_i}{\bar{l}} \rceil$ sub-partitions. Each sub-partition contains b^2 blocks, and each block holds \bar{l} edges, protecting the variance among the data providers.

Step 2 - MPC servers globally integrate the private partitions.

After dividing the private graph G_i into s_i ($b \times b \times \bar{l}$) sub-partitions, P_i encrypts all elements, including all IDs and attributes, into boolean secret shares and sends the shares to the computation servers. Each encrypted and transferred partition is a $(b \times b \times \bar{l})$ secret matrix and is indistinguishable from the others, we refer to it as $\llbracket G_u.\text{Block} \rrbracket$.

The data providers send each $\llbracket G_u.\text{Block} \rrbracket$ through a separate anonymous channel, authorized via the *ring signature* [52]. This ensures that the computation servers only receive $N^+ = \sum_{i=1}^N s_i$ secret $\llbracket G_u.\text{Block} \rrbracket$ s, but cannot identify which one comes from which

data provider. The servers then run b^2 secure *odd_even_merge_sort* networks concurrently to merge blocks from each $\llbracket G_u.\text{Block} \rrbracket$, thereby constructing the global secret partitioned graph, $\llbracket G.\text{Block} \rrbracket$. The size of $\llbracket G.\text{Block} \rrbracket$ is $(b \times b \times l)$, where $l = \sum_{i=1}^{N^+} \bar{l}$.

Step 3 - MPC servers construct secure index. To enable secure and efficient access to the target partition for each query, GORAM builds the partitions as ORAMs. Specifically, we model the partitioned graph $\llbracket G.\text{Block} \rrbracket$ with two ORAMs for vertex- and edge-centric queries: (1) VORAM models $\llbracket G.\text{Block} \rrbracket$ as an array (Arr) of b partitions, each is one row of b blocks; and (2) EORAM models $\llbracket G.\text{Block} \rrbracket$ as an array of b^2 partitions, each is an edge block. The indices of EORAM are the flattened indices of the blocks, i.e., the index of block (i, j) is $ib + j$.

The two sub-ORAMs are initialized in the following way, similar to ORAM: (1) shuffling the graph in the unit of partitions according to a random permutation π to construct $ShufArr$, and storing the secret permutation representation $\llbracket \pi \rrbracket$. We refer to this procedure as *ShuffleMem*, which is the primary bottleneck during GORAM initialization. To enhance the efficiency, Section 4.4 provides a constant-round *ShuffleMem* for the underlying $(2, 3)$ -secret shares. (2) constructing the index map that translates the logical index $[i]$ into a physical index p pointing to the target partition of $ShufArr$, where Arr_i and $ShufArr_p$ refer to the same partition. The construction phase follows the same procedure as ORAM (see Section 4.1).

Access the partition. After the initialization, the MPC servers can jointly access GORAM as follows:

(1) Given the target vertex $[v]$ (from the clients), the servers can compute the partition index $\llbracket \lceil \frac{v}{k} \rceil \rrbracket$ and obtain the partition containing bl secret edges by accessing VORAM. This partition contains *all* the direct neighbors of $[v]$.

(2) Given the target edge $([v_s], [v_d])$, the servers can compute the partition index $\llbracket \lceil \frac{v_s}{k} \rceil * b + \lceil \frac{v_d}{k} \rceil \rrbracket$ and obtain the partition containing l secret edges by accessing EORAM. This partition contains *all* edges $([v_s], [v_d])$ of the global graph if the edges exist.

For each given query, the servers only need to access one partition and scan the single partition to obtain the result (see Section 5). Thus, the query processing complexity is sublinear.

Batched update. To update GORAM, each data provider can locally update the private graph G_i and send the updated edge blocks to the computation servers. The servers then update the corresponding edge blocks in the global graph $\llbracket G.\text{Block} \rrbracket$ and re-construct the secure index, similar to the construction procedure.

4.3 Parallelization and Vectorization

GORAM is a *parallel-friendly* data structure. All stages in its lifecycle can be accelerated through parallel processing.

In the local process stage, each data provider can independently split the private graph G_i into the 2d-partitioned format, during which the edge blocks can be processed in parallel. During the global integration, the primary bottleneck, i.e., the *odd_even_merge_sort* of b^2 edge blocks from N^+ secret graphs $\{\llbracket G_u.\text{Block} \rrbracket\}_{i=1}^{N^+}$, can be performed in at most b^2 tasks in parallel. After obtaining the $b \times b \times l$ global graph partitions, we can split it into p *partition slices* for arbitrary $p \leq l$ because each edge block is a list of l edges that can be processed in parallel. Specifically, we split the $b \times b$ edge blocks by edges into p $b \times b \times l^{(j)}$ partition slices, $l = \sum_{j=1}^p l^{(j)}$. Each

²A sorted order is beneficial for some queries, as discussed in Section 5.

$S1(A, B)$	$S2(B, C)$	$S3(C, A)$
0) Construct the shares of $L = [n]$.		
$L_A = Z_1 \oplus L$	$L_B = Z_2$	$L_C = Z_3$
$\leftarrow L_A$	$\leftarrow L_B$	$\leftarrow L_C$
1) Prepare the correlated randomness.		
$Z_{12}, Z_{12}^L, \tilde{B}$ π_{12} and π_{12}^{-1}	$Z_{12}, Z_{12}^L, \tilde{B}$ π_{12} and π_{12}^{-1}	$Z_{23}, Z_{23}^L, \tilde{L}_C$ π_{23} and π_{23}^{-1}
$Z_{31}, Z_{31}^L, \tilde{A}, \tilde{L}_A$ π_{31} and π_{31}^{-1}	$Z_{23}, Z_{23}^L, \tilde{L}_C$ π_{23} and π_{23}^{-1}	$Z_{31}, Z_{31}^L, \tilde{A}, \tilde{L}_A$ π_{31} and π_{31}^{-1}
2) Main protocol: computation and communications		
$X_1 = \pi_{12}(A \oplus B \oplus Z_{12})$ $X_2 = \pi_{31}(X_1 \oplus Z_{31})$	$Y_1 = \pi_{12}(C \oplus Z_{12})$ $LY_1 = \pi_{23}^{-1}(L_B \oplus Z_{23}^L)$	$LX_1 = \pi_{23}^{-1}(L_C \oplus L_A \oplus Z_{23}^L)$ $LX_2 = \pi_{31}^{-1}(LX_1 \oplus Z_{31}^L)$
$X_2 \leftrightarrow LY_1$	$Y_1 \leftrightarrow LX_2$	
$LY_2 = \pi_{31}^{-1}(LY_1 \oplus Z_{31}^L)$ $LY_3 = \pi_{12}^{-1}(LY_2 \oplus Z_{12}^L)$ $L_{B_1} = LY_3 \oplus L_A$	$X_3 = \pi_{23}(X_2 \oplus Z_{23})$ $\tilde{C}_1 = X_3 \oplus \tilde{B}$ $LX_3 = \pi_{12}^{-1}(LX_2 \oplus Z_{12}^L)$ $L_{B_2} = LX_3 \oplus L_C$	$Y_2 = \pi_{31}(Y_1 \oplus Z_{31})$ $Y_3 = \pi_{23}(Y_2 \oplus Z_{23})$ $\tilde{C}_2 = Y_3 \oplus \tilde{A}$
$L_{B_1} \leftrightarrow L_{B_2}$	$\tilde{C}_1 \leftrightarrow \tilde{C}_2$	
$\tilde{L}_B = \tilde{L}_{B_1} \oplus \tilde{L}_{B_2}$	$\tilde{L}_B = L_{B_1} \oplus L_{B_2}$	
3) Output		
$\tilde{A}, \tilde{B}, \tilde{L}_A, \tilde{L}_B$	$\tilde{B}, \tilde{C}, \tilde{L}_B, \tilde{L}_C$	$\tilde{C}, \tilde{A}, \tilde{L}_C, \tilde{L}_A$

Protocol 1: ShuffleMem Build Protocol $\Pi_{\text{ShufMem}} - \text{Lightgray}$ operations are our extensions of Araki et al. [10] to compute $\llbracket \tilde{\pi} \rrbracket$.

slice contains all the edge blocks but fewer edges per block. We can then establish p secure indices for each partition slice concurrently. For each query, the p partition slices can be accessed and processed in parallel, and each slice can be processed as a single vector for better performance (Section 5). The query result can be obtained by merging the results of p partition slices.

4.4 Optimization on ShuffleMem Step

The most expensive step during GORAM initialization is the ShuffleMem procedure in secure index construction, which shuffles the array according to a random permutation π and stores the secret permutation representation $\llbracket \tilde{\pi} \rrbracket$. For an array with n partitions, the original ShuffleMem (i.e., *Waksman permutation network* adopted in [66]) incurs $O(n \log n)$ communication and computation, which is expensive for large n . To optimize this, GORAM designs a constant-round $O(n)$ ShuffleMem to accelerate the initialization process by extending Araki et al. [10] on (2, 3)-secret shares.

The ShuffleMem procedure. The computation servers begin with a secret shared array $\llbracket D \rrbracket = \{\llbracket D_0 \rrbracket, \llbracket D_1 \rrbracket, \dots, \llbracket D_{n-1} \rrbracket\}$ of n partitions. At the end of the protocol, the computation servers output two secret shared arrays $\llbracket \tilde{D} \rrbracket$ and $\llbracket \tilde{\pi} \rrbracket$, where \tilde{D} is a permutation of D under some random permutation π and $\llbracket \tilde{\pi} \rrbracket$ is the secret-shared permutation representation of π . The permutation π is a bijection mapping from D to itself that moves the i th partition D_i to place $\pi(i)$. The permutation result $\tilde{D} = \{\tilde{D}_0, \tilde{D}_1, \dots, \tilde{D}_{n-1}\} = \pi(D)$ satisfies that $D_i = \tilde{D}_{\pi(i)}, \forall i \in \{0, 1, \dots, n-1\}$. The permutation representation $\tilde{\pi}$ is an array of n elements that explicitly records the location of each D_i in \tilde{D} in its i th element $\tilde{\pi}_i$.

Key idea of constant-round construction. We design the constant-round ShuffleMem by extending the constant-round shuffle protocol of Araki et al. [10], which computes $\llbracket \tilde{D} \rrbracket$ in $O(n)$ complexity and $O(1)$ communication rounds using (2, 3)-secret sharing.

The key idea of our protocol is to compute $\llbracket \tilde{\pi} \rrbracket$ simultaneously by leveraging the properties of permutations:

- * Permutations are composable, i.e., $\pi_1 \circ \pi_2$ is also a permutation such that $(\pi_1 \circ \pi_2)(x) = \pi_1(\pi_2(x))$ given array x .
- * Permutations are inversible, for each permutation π , there exists π^{-1} such that $(\pi^{-1} \circ \pi)(x) \equiv x$.
- * The permutation representation $\tilde{\pi} = \pi^{-1}(L)$, where $L = \{0, 1, \dots, n-1\}$, n is the size of x .

Specifically, Araki et al. [10] implement the random shuffle by letting the computation servers collaboratively shuffle the data using three random permutations π_{12}, π_{23} and π_{31} , i.e., $\llbracket \tilde{D} \rrbracket = \pi_{23} \circ \pi_{31} \circ \pi_{12}(\llbracket D \rrbracket) = \pi(\llbracket D \rrbracket)$. The permutation π_{ij} is only known to servers S_i and S_j . Because each computation server only knows two out of the three random permutations, the overall permutation $\pi = \pi_{23} \circ \pi_{31} \circ \pi_{12}$ remains random for each computation server. Using the same collaborative shuffle procedure, we can compute the secret permutation representation $\llbracket \tilde{\pi} \rrbracket$ simultaneously by shuffling the ranging array $L = \{0, 1, \dots, n-1\}$ using the inverse permutations i.e., $\llbracket \tilde{\pi} \rrbracket = \pi^{-1}(\llbracket L \rrbracket) = \pi_{12}^{-1} \circ \pi_{31}^{-1} \circ \pi_{23}^{-1}(\llbracket L \rrbracket)$.

ShuffleMem construction. Protocol 1 shows the ShuffleMem construction. Each pair of computation servers S_i and S_j share a common random seed $s_{i,j}$ beforehand. As inputs to this protocol, each computation server holds two out of the three shares A, B, C , satisfying that the input $D \equiv A \oplus B \oplus C$. Also, the computation servers construct the shares of the ranging array $L \equiv L_A \oplus L_B \oplus L_C$, which requires one round of communication. Specifically, S_1, S_2 and S_3 at first construct an array of secret shares on zeros, i.e., $Z_1 \oplus Z_2 \oplus Z_3 \equiv \vec{0}$, $|\vec{0}| = n$, which requires no interactions using [49]. Each Z_i is uniformly random and is only known to S_i . S_1 locally computes $L_A = Z_1 \oplus L$ and each server sends its share to the previous server to obtain the secret shares of L (step 0). The first step of Protocol 1 is to set up the correlated randomness using the pairwise random seed. Also, each pair of S_i and S_j generates a random permutation $\pi_{i,j}$ and the inverse permutation $\pi_{i,j}^{-1}$.

The computation servers then begin the main protocol, during which there are two invariants held: 1) $X_i \oplus Y_i$ is a permutation of D and 2) $LX_i \oplus LY_i$ is an inverse permutation of L . For examples, $X_1 \oplus Y_1 = \pi_{12}(A \oplus B \oplus Z_{12}) \oplus \pi_{12}(C \oplus Z_{12}) = \pi_{12}(A \oplus B \oplus C) = \pi_{12}(D)$, $LY_1 \oplus LX_1 = \pi_{23}^{-1}(L_B \oplus Z_{23}^L) \oplus \pi_{23}^{-1}(L_C \oplus L_A \oplus Z_{23}^L) = \pi_{23}^{-1}(L)$. That is, during the main protocol, the servers sequentially compute $X_1 \oplus Y_1 = \pi_{12}(D)$, $X_2 \oplus Y_2 = (\pi_{31} \circ \pi_{12})(D)$ and $X_3 \oplus Y_3 = (\pi_{23} \circ \pi_{31} \circ \pi_{12})(D)$, which constitutes the final shares of $\pi(D)$, $\pi = \pi_{23} \circ \pi_{31} \circ \pi_{12}$. The permutation representation $\tilde{\pi} = \pi^{-1}(L) = (\pi_{12}^{-1} \circ \pi_{31}^{-1} \circ \pi_{23}^{-1})(L)$ is constructed similarly in the reverse order.

Correctness. From the two invariants, it is straightforward to see the correctness of ShuffleMem Protocol 1. Because the final shares satisfy that $\tilde{A} \oplus \tilde{B} \oplus \tilde{C} = \tilde{X}_3 \oplus \tilde{Y}_3 = \pi(D)$, and $\tilde{L}_A \oplus \tilde{L}_B \oplus \tilde{L}_C = \tilde{L} \tilde{X}_3 \oplus \tilde{L} \tilde{Y}_3 = \pi^{-1}(L)$, the correctness is guaranteed.

Security. Protocol 1 satisfies Theorem 1. We provide a sketch proof here and the complete proof is shown in Appendix A.1.

THEOREM 1. *Protocol 1 securely implements the ShuffleMem procedure against any semi-honest adversary controlling at most one computation server.*

PROOF. (sketch) We prove Theorem 1 with the *real-ideal* paradigm [21]. Let \mathcal{A} denotes the real-world adversary and \mathcal{S} denotes

Algorithm 1: EdgeExist (MPC servers compute)

Inputs : Target edge $([v_s], [v_d])$.
Output : $[\text{flag}]$ indicating whether the target edge exist in global G .

- 1 Compute the secret partition ID $[i] = \lceil \lceil \frac{v_s}{k} \rceil * b + \lceil \frac{v_d}{k} \rceil \rceil$;
- 2 Fetch the target edge partition $[B] \leftarrow \text{EORAM.access}([i])$, where $[B]$ contains l source_nodes and dest_nodes;
// Vectorized edges comparisons.
- 3 Construct $[\vec{v}_s]$ and $[\vec{v}_d]$ by expanding $[v_s]$ and $[v_d]$ l times;
- 4 Compute $[\text{mask}_s] \leftarrow \text{EQ}([\vec{v}_s], [B].\text{source_nodes})$;
- 5 Compute $[\text{mask}_d] \leftarrow \text{EQ}([\vec{v}_d], [B].\text{dest_nodes})$;
- 6 Compute $[\text{mask}] \leftarrow \text{AND}([\text{mask}_s], [\text{mask}_d])$;
// Aggregating the result through OR.
- 7 **while** $\text{len}([\text{mask}]) > 1$ **do**
 - 8 Pad $[0]$ to $[\text{mask}]$ to be even ;
 - 9 Split $[\text{mask}]$ half-by-half to $[\text{mask}]_l$ and $[\text{mask}]_r$;
 - 10 Aggregate $[\text{mask}] \leftarrow \text{OR}([\text{mask}]_l, [\text{mask}]_r)$;
- 11 **end**
- 12 Compute $[\text{flag}] = [\text{mask}]$;
- 13 **return** $[\text{flag}]$ to the client.

Algorithm 2: NeighborsCount (MPC servers compute)

Inputs : Target vertex $[v]$.
Output : $[\text{num}]^A$, the number of v 's outing neighbors.

- 1 Compute the secret partition ID $[i] = \lceil \lceil \frac{v}{k} \rceil \rceil$;
- 2 Fetch the target edge partition $[B] \leftarrow \text{VORAM.access}([i])$, where $[B]$ contains (bl) source_nodes and dest_nodes;
// Filtering real neighbors using vectorization.
- 3 Construct $[\vec{v}]$ by expanding $[v]$ bl times;
- 4 Compute $[\text{mask}] \leftarrow \text{EQ}([\vec{v}], [B].\text{source_nodes})$;
- 5 Obtain the arith shares $[\text{mask}]^A \leftarrow \text{B2A}([\text{mask}])$;
// Counting real neighbor masks.
- 6 Compute $[\text{num}]^A \leftarrow \text{SUM}([\text{mask}]^A)$;
- 7 **return** $[\text{num}]^A$ to the client.

the simulator, which simulates the view of \mathcal{A} in the ideal world. Protocol 1 is secure if for all \mathcal{A} , there exists a simulator \mathcal{S} , such that for all inputs and for all corrupted party $S_i, i \in [3]$,

$$\text{View}(\mathcal{A}) \equiv \text{View}(\mathcal{S}) \quad (1)$$

For each possible corrupted S_i , all the messages it receives are uniformly random in its view. This is achieved by masking all the messages S_i receives with at least one randomness that S_i does not know. Therefore, we can construct the simulator \mathcal{S} by randomly sampling all the messages that \mathcal{A} receives. The $\text{View}(\mathcal{S})$ is uniformly random and therefore indistinguishable from $\text{View}(\mathcal{A})$. \square

5 Querying Graphs through GORAM

We provide five ego-centric query examples through GORAM, covering all queries listed in LinkBench [11]. The other queries can be similarly achieved. For each query, the client submits the secret query key to the servers. The servers process the queries and return the secret shares of the results to the client. Only the client can reconstruct the plaintext final result.

Algorithm 3: NeighborsGet (MPC servers compute)

Inputs : Target vertex $[v]$.
Output : $[\text{neighbors}]$, the unique outing neighbor's IDs of $[v]$.

- 1 Compute the secret partition ID $[i] = \lceil \lceil \frac{v}{k} \rceil \rceil$;
- 2 Fetch the target edge blocks $[B] \leftarrow \text{VORAM.access}([i])$, where $[B]$ contains (bl) source_nodes and dest_nodes;
// 1) Filtering real neighbors.
- 3 Construct $[\vec{v}]$ by expanding $[v]$ bl times;
- 4 Compute $[\text{mask}] \leftarrow \text{EQ}([\vec{v}], [B].\text{source_nodes})$;
- 5 Compute $[\text{candidate}] \leftarrow \text{MUL}([\text{mask}], [B].\text{dest_nodes})$;
// 2) De-duplicating neighbors.
- 6 $[\text{same_mask}] \leftarrow \text{NEQ}([\text{candidate}]_{[1:]}, [\text{candidate}]_{[-1:]})$;
- 7 Compute $[\text{same_mask}].\text{append}([1])$;
- 8 Compute $[\text{neighbors}] \leftarrow \text{MUL}([\text{same_mask}], [\text{candidate}])$;
- 9 Compute $[\text{neighbors}] \leftarrow \text{SHUFFLE}([\text{neighbors}])$;
- 10 **return** $[\text{neighbors}]$ to the client.

5.1 Basic Queries

EdgeExist Algorithm 1 is a basic query that checks whether an edge (v_s, v_d) exists. We first access EORAM using secret index $\lceil \lceil \frac{v_s}{k} \rceil * b + \lceil \lceil \frac{v_d}{k} \rceil \rceil$. Then, we compare all the edges in the partition using vectorization. The comparison result is a secret $[\text{mask}]$ indicating which edge is equivalent to the given edge. We obtain the result by aggregating $[\text{mask}]$ using the OR operation.

NeighborsCount Algorithm 2 counts the number of target vertex v 's outing neighbors. Because the query is about vertex v , we refer to VORAM for the partition containing all its outing neighbors using secret index $\lceil \lceil \frac{v}{k} \rceil \rceil$. We obtain the result by comparing all starting vertices to v and summing up the comparison result. For efficiency, we transform $[\text{mask}]$ to arithmetic shares, i.e., $[\text{mask}]^A$, which enable summation without communications.

NeighborsGet Algorithm 3 extracts all the 1-hop outing neighbors of the target vertex v while maintaining the number of edges between each neighbor and v private. The first 3 lines access the target partition and compare all the starting vertices with v to construct $[\text{mask}]$, indicating the edges started from v . Then, we multiply the $[\text{mask}]$ and the destination vertices to obtain $[\text{candidate}]$, where each element is $[0]$ or $[u]$ if u is an outing neighbor of v . Note that the number of $[u]$ implies the number of edges between u and v , we then de-duplicate $[\text{candidate}]$ in lines 5-8 to mask out this information. Because each partition is sorted by key $v||u$ in the construction stage (see Section 4.2), all the same outing neighbors in $[\text{candidate}]$ are located successively as a group. We apply a shifted NEQ on $[\text{candidate}]$ to compute $[\text{same_mask}]$, where only the last neighbor in each group is $[1]$, while the rest are $[0]$. By multiplying $[\text{same_mask}]$ and $[\text{candidate}]$, we mask out the duplicate neighbors as $[0]$. Note that the gap between two successive neighbors u_i, u_{i+1} still implies how many u_{i+1} exist, and therefore, we apply SHUFFLE to permute this location-implied information.

5.2 Complex queries

We provide two complex queries by extending the above queries.
Cycle-identification. Identifying whether the bank transactions across multiple suspicious accounts form a cycle is an effective way for money laundering detection [45, 53]. Cycle identification can be

Table 1: Complexity Summarization (see Appendix B for detailed derivation.)

Data Structures		Initialization		Partition Access		Partition Processing for Basic Queries					
						EdgeExist		NeighborsCount		NeighborsGet	
		Comp	Round	Comp	Round	Comp	Round	Comp	Round	Comp	Round
Mat	adj-VORAM	$O(N V ^2)$	$3 + 2\log_P(\frac{ V }{T})$	$O(PT \log_P(\frac{ V }{T}))$	$O(\log_P(\frac{ V }{T}))$	$O(1)$	$O(1)$	$O(V)$	$O(1)$	$O(V)$	$O(1)$
	adj-EORAM		$3 + 2\log_P(\frac{ V ^2}{T})$	$O(PT \log_P(\frac{ V ^2}{T}))$	$O(\log_P(\frac{ V ^2}{T}))$						
List		$O(E \log(E) \log(N))$	$\log(E) \log(N)$	$O(1)$	NA	$O(E)$	$O(\log(E))$	$O(E)$	$O(1)$	$O(E)$	$O(1)$
GORAM	VORAM	$O(b^2 l \log(l) \log(N^+))$	$3 + \log(l) \log(N^+) + 2\log_P(\frac{b}{T})$	$O(PT \log_P(\frac{b}{T}))$	$O(\log_P(\frac{b}{T}))$	$O(l)$	$O(\log(l))$	$O(bl)$	$O(1)$	$O(bl)$	$O(1)$
	EORAM		$3 + \log(l) \log(N^+) + 2\log_P(\frac{b^2}{T})$	$O(PT \log_P(\frac{b^2}{T}))$	$O(\log_P(\frac{b^2}{T}))$						

P and T denote the pack and stash size of ORAM. b, l are the configuration parameters of 2d-partition, where $b = \frac{|V|}{k} = \frac{|E|}{|V|} = D$ is the graph density. The Round complexities with the $O(\cdot)$ notation is in the unit of secure operations like EQ, and the Partition Access complexities are the averaged complexity of successive T queries. $N \geq 1$ is the number of data providers. N^+ is the number of all the submitted partitions, $N^+ \geq N$.

achieved by submitting a series of EdgeExist queries. For example, given three vertices v_1, v_2 and v_3 , by submitting EdgeExist queries on edges $(v_1, v_2), (v_2, v_3), (v_3, v_1)$ and their reverse edges, the client can detect whether a cycle exists among the three vertices.

Neighbors-filtering queries are one of the most common queries on graphs with attributes, i.e., each edge has attributes like creation timestamp and transaction amounts. We can implement these queries by extending the basic queries with filters. For instance, to perform *association range queries* [11] that count the outing edges created after a provided timestamp, we can extend NeighborsCount with an extra comparison to compute whether the creation timestamp is greater than the given timestamp before counting the result. Specifically, we compute $\llbracket t_mask \rrbracket \leftarrow GT(\llbracket timestamp\ field \rrbracket, \llbracket given\ threshold \rrbracket)$ and update the neighbors mask in the 3rd line of Algorithm 2 to $\llbracket mask \rrbracket = AND(\llbracket mask \rrbracket, \llbracket t_mask \rrbracket)$. Then we obtain the number of outing edges created after the given timestamp.

6 Security and Complexity Analysis

6.1 Security Analysis

We illustrate the security guarantees of GORAM by showing that no involved party (data providers, clients, and computation servers) can learn anything about the private graphs and the query keys.

(1) Data providers learn nothing about the others' private graphs or the query keys because they only submit secret-shared graph partitions to the servers.

(2) Clients learn nothing about the data providers' graphs or the other keys because they only submit secret-shared keys to the servers and receive results obtained from the global graph.

(3) During GORAM initialization and query process, the computation servers only execute MPC protocols on N^+ indistinguishable $b \times b \times \bar{l}$ secret-shared partitioned graph matrices and secret-shared query keys. These protocols are executed in the standard *modular composition* manner [21], which ensures that the overall computation performed by the servers inherits the same security guarantees of the underlying protocols. This includes the ABY3 protocols [49] and the proposed ShuffleMem protocol, whose security is proved in Section 4.4. Consequently, the only potential source of private information for the servers is the sizes of the input matrices, i.e., b ,

\bar{l} and the total matrices number N^+ . Among these, \bar{l} is a public parameter, and $b = \lceil \frac{|V|}{k} \rceil$ is derived from two public parameters, $|V|$ and k . The number of the matrices, N^+ , only reveals the partition size of the global graph and cannot be traced back to any specific data provider because of the anonymous authentication property provided by ring signature. Therefore, both the private graphs and the query keys are protected throughout the lifecycle of GORAM.

6.2 Complexities Analysis

Complexity summarization. Table 1 summarizes the complexities of initialization, partition access, and basic query processing using GORAM and the strawman solutions. The complexities are directly derived from the algorithms of their respective sections. Specifically, GORAM's initialization is bottlenecked by the $O(b^2 l \log(l) \log(N^+))$ merge sort on N^+ partitioned graphs (Section 4.2). Partition access has an ORAM access complexity of $O(PT \log_P(\frac{b}{T}))$ or $O(PT \log_P(\frac{b^2}{T}))$ for VORAM and EORAM, respectively (Section 4). Partition processing is linear to the partition size (Section 5.1). The discussion of complexities on *Mat* and *List* is left to Section 7.1, and Appendix B provides the detailed derivation.

Partition size l analysis. We analyze the distributions of the partition size l across five distributed graphs using the *Monte Carlo* method. Our findings in Section 7.3 indicate that, across all distributions, the partition size l lies in a small range and is notably smaller than the total edge count, i.e., $l \ll |E|$, indicating that GORAM can effectively process queries by accessing only one partition. The worst-case partition size $l = |E|$ is *unlikely* in practice because it requires: (1) all the edges in the graph only involve at most $2k$ vertices, k for starting vertices and k for the endings, and (2) the graph forms a bipartite graph starting from and ending in two chunks after the *random* permutation in the initialization stage (Section 4).

7 Evaluation

We evaluate GORAM on a variety of graphs and queries to demonstrate its scalability and performance.

7.1 Evaluation Setup

Setup. We implement the GORAM prototype based on ABY3 [49], a popular 3-party MPC platform. We use three computation servers on the cloud, each equipped with $16 \times 2.0\text{GHz}$ Intel CPU cores,

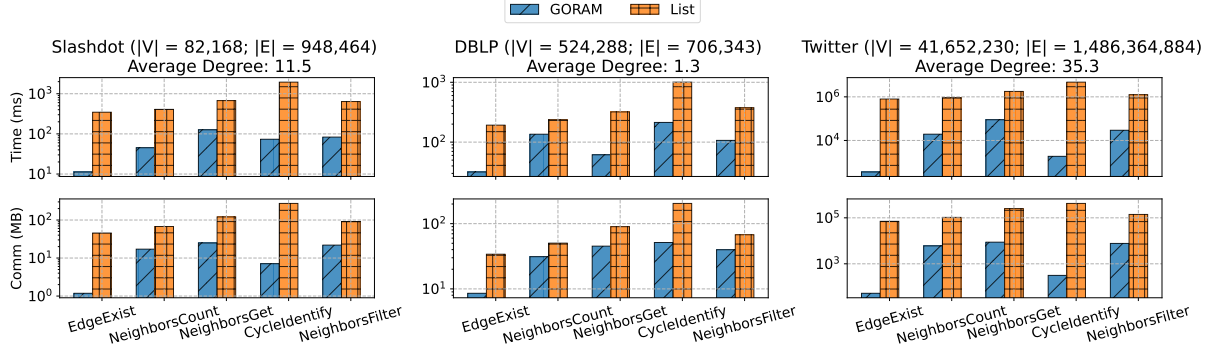


Figure 4: Queries on Real-world Graphs * the y-axes are in log-scale. Queries on Twitter are in 16 threads and the others are single-threaded.

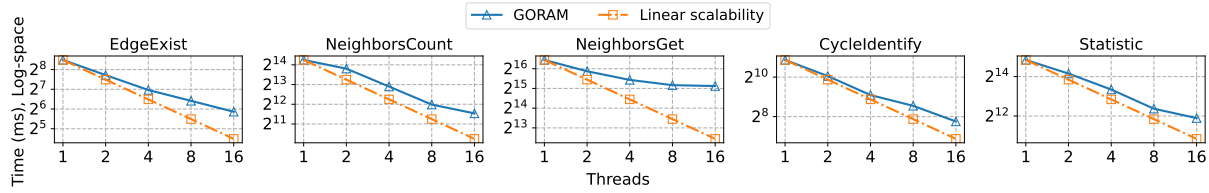


Figure 5: Parallelism on Twitter [18] (Queries)

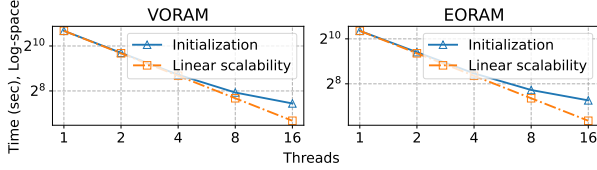


Figure 6: Parallelism on Twitter [18] (Initialization)

512GB memory and 10Gbps full duplex Ethernet with an average round-trip-time (RTT) of 0.12 ms. Note that we use the entire memory just to support a larger-scale *Mat* baseline.

Workload. We use graphs of two types over all five queries in Section 5. First, we use three open-source real-world graphs, including Slashdot [6], DBLP [63], and Twitter [18], with the number of edges ranging from less than 1 million to more than 1 billion. Figure 4 in Section 7.2 lists the key parameters of these graphs. To show the detailed performance characteristics of GORAM, we also use thirty synthetic graphs of five different edge distributions from igraph [32]. For each distribution, we range the number of vertices $|V|$ from 1K to 32K. Table 2 in Section 7.3 summarizes the key parameters of these graphs.

Strawman solutions for comparison. Since there are no systems known to us that can provide the same functionality as GORAM, we implement the strawman solutions in Section 3.2, upon which we also implement the same five queries. We fine-tune the performance to add vectorization and parallelism, wherever applicable, making sure that the performance difference from implementation quality is minimized. In fact, much of the low-level code is shared with GORAM, including the ORAM and all the secure protocols.

For *Mat*, we first implement the three basic queries as follows: 1) *EdgeExist* query on edge $([v_i], [v_j])$: we directly extract the element (i, j) using the adj-EORAM (Section 3.2) and compare it to 0; 2) *NeighborsCount*: we access adj-VORAM and sum up the number of

edges; and 3) *NeighborsGet*: we access adj-VORAM, and compare the elements with 0 through GT operator to hide the exact number of edges, and then return the result to the client. The *CycleIdentify* is then implemented by composing six *EdgeExist*, the same as GORAM. We ignore the *NeighborsFilter* query because *Mat* can not support multi-graphs, as we analyzed in Section 3.2. For *List*, we implement all queries by scanning the whole edge list, reusing GORAM’s implementation on each partition.

Execution time measurements. All the reported execution times are the wall-clock time measured on the computation servers from the start to the end of the initialization or query processing. We report the average from 5 runs. For GORAM and *Mat* that require ORAM accesses, the query processing time is the averaged time of successive T queries³, where T is the stash size, and we use $T = \sqrt{\#(\text{items in ORAM})}$, the default setting in [66].

7.2 Performance on Real-world Graphs

We first provide an overview of GORAM performance using three real-world graphs with 700K to 1.4 billion edges.

Overall Query Performance. The first row of Figure 4 shows the query execution time for five queries. The configuration parameters k and \bar{l} are the default values stated in Section 4. For each query, we use the maximum vector size. We use single-threading for smaller graphs and 16 threads for the larger Twitter graph.

For smaller Slashdot [6] and DBLP [63], GORAM completes all the queries within 135.7 ms. To our knowledge, this is the only system that supports sub-second ego-centric queries on these graphs with strong privacy guarantees. In comparison, *Mat* gets out of memory even with the entire 512GB of memory per server, and *List* is 15.9× and 4.2× slower on average on these two graphs.

³For static queries, we can initialize fresh ORAMs in background processes and directly use a fresh ORAM when the stash is full.

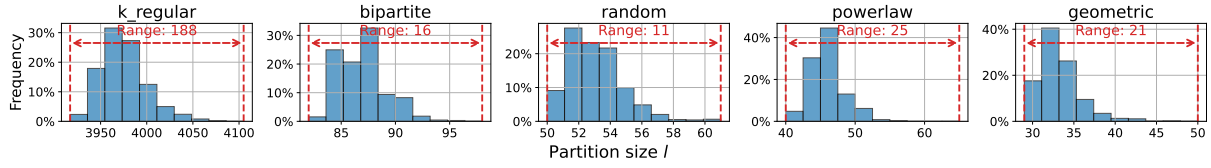


Figure 7: Distribution of Partition Size l on Varied Distributed Graphs ($|V| = 32K$).

For the large Twitter, GORAM only takes 58.1 ms to 35.7 seconds to complete all queries, achieving a remarkable average speedup of $473.5\times$ over *List*. Across all queries, we find that GORAM achieves more significant speedups for EdgeExist and CycleIdentify, with $856.3\times$ and $1445.6\times$ speedups, respectively. This is because these two queries use the EORAM, with which we only need access *one* of the $b^2 = 4096$ edge blocks with 1.1M edges, which is less than 0.8% of the total edges. Instead, the other three use the VORAM that accesses one *row* of the $b = 64$ edge blocks, which contain 71.2M edges, accounting 4.9% for the total edges.

Fast query execution comes from processing less data. To verify that the execution time reduction indeed comes from reduced computation through partitioning, we also measure the total bytes transferred in each query on each graph. The second row in Figure 4 shows the results, which are consistent with execution time - we observe an average communication reduction of 78.4% compared to *List*. Also, the maximum reduction of 99.9% is observed in EdgeExist and CycleIdentify, for the same reason above.

Fast query execution also comes from parallel execution. Query performance on large graphs also benefits from parallelization, as shown in Figure 5. On the large Twitter, we observe that using 16 threads, we can achieve an average speedup of $6.3\times$ across the five queries over a single thread. We observe that except for NeighborsGet, we can achieve almost linear scalability using up to 16 threads. The slight derivation from linear scalability is because 8 threads already accelerate the computation to sub-second levels; adding more threads provides minimal speedup while increasing the aggregation overhead. NeighborsGet does not parallel well because the SHUFFLE procedure (line 8 in Algo. 3) needs to process the entire partition to permute the result, which is inherently sequential.

Initialization performance. Unlike *List*, both VORAM and EORAM require a non-trivial initialization step to construct the secure indices (Section 4.2). While the two smaller graphs only take a few seconds, it takes dozens of minutes on the large Twitter using a naive sequential algorithm. However, we can parallelize the initialization using multiple threads, as shown in Section 4.3. In this way, we can construct both VORAM and EORAM for the billion-edge-scale graph within 2.9 minutes using 16 threads. Figure 6 shows the experiments using different numbers of threads. We observe an average speedup with 16 threads is $9.4\times$ over a single thread, and at this setting, we have saturated the 10Gbps network bandwidth.

7.3 Micro-benchmarks

To better understand GORAM performance, we run queries on 30 synthetic graphs of various distributions and sizes, measure the execution time, and compare to the two strawman solutions. Limited by space, we only present three basic queries NeighborsCount,

Table 2: Synthetic Graphs

Graph Types	Generation Methods	Average Degree
k_regular	K-Regular [1]	7.5
bipartite	Random_Bipartite [2]	134.4
random	Erdos_Renyi [3]	268.8
powerlaw	Barabasi [4]	523.7
geometric	GRG [5]	1198.5

Table 3: Parameters of Synthetic Graphs with $|V|=32K$

Graph Type	$ E $	k	b	l	bl	$b^2l/ E $
k_regular	0.2M	4096	8	3960	31.8K	1.03
bipartite	13.4M	64	512	88	44.5K	1.72
random	26.8M	32	1024	56	57.3K	2.19
powerlaw	52.3M	16	2048	48	98.3K	3.85
geometric	105.0M	8	4096	32	131.1K	5.11

The parameters k , b and l refer to # (vertices per chunk), # (vertex chunks) and the edge block size with padded edges, see Section 4. l and bl are the EORAM and VORAM partition sizes, respectively.

NeighborsGet and EdgeExist, because the other two are based on these queries and thus CycleIdentify offers similar performance as EdgeExist, and NeighborsFilter is similar to NeighborsCount. We focus on single-thread-only for all micro-benchmarks to best illustrate the performance benefit from the GORAM data structure.

Adaption to various distributed graphs. Each distribution of the graph presents a different density, i.e. vertex degree $D = \frac{|E|}{|V|}$, with the average degree shown in Table 2. Among them, the k_regular is the sparsest and the geometric is the densest. We present the default configuration parameters k of GORAM (see Section 4) and the corresponding vertex chunk numbers b , the partition sizes for EORAM (l) and VORAM (bl) in Table 3. The ratio $\frac{b^2l}{|E|}$ is also shown, representing the amplification factor of the 2d-partitioned structure with padded edges for security compared to the original edge list. We observe that for sparse k_regular, GORAM uses k as large as 4096, while for geometric, k gets as small as 8. The choice of k makes intuitive sense. Recall that a key property when we partition is that all outgoing edges of a vertex are within a single row of the 2d-partition. Thus, when the graph is sparse, we have the opportunity to partition it into fewer chunks, i.e., smaller $b = \frac{|V|}{k}$, enjoying the benefits from quicker partition access time. However, on a dense graph, we partition it into more chunks to make each partition smaller, thereby reducing the partition scanning time per query.

Partition size l distributions across diverse distributed graphs are shown in Figure 7, derived through the *Monte Carlo* method. For each distribution, we generate 10K graphs, each with 32K vertices. For each graph, we randomly permute the vertices using different

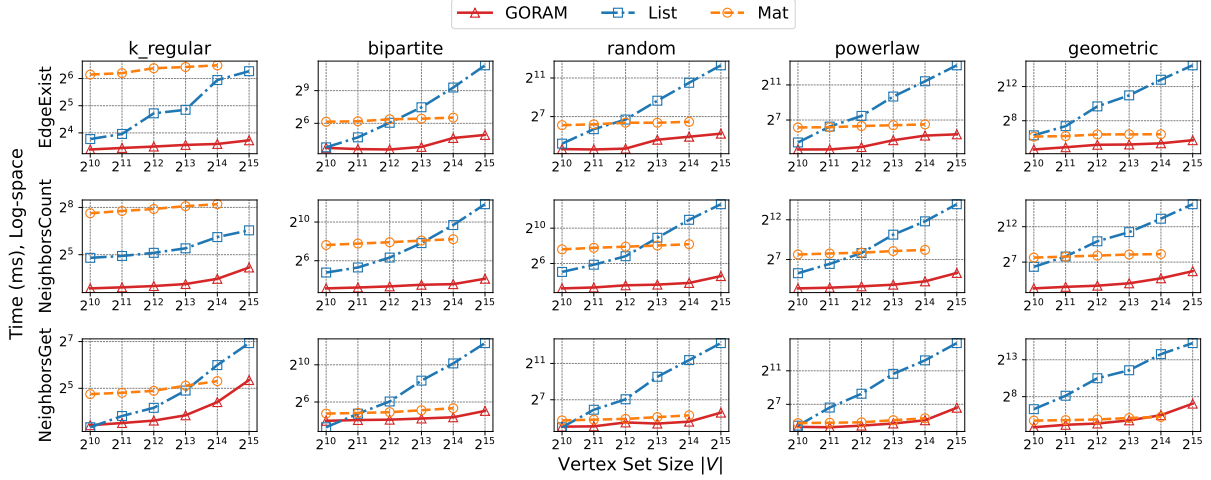


Figure 8: Online Performance Overview

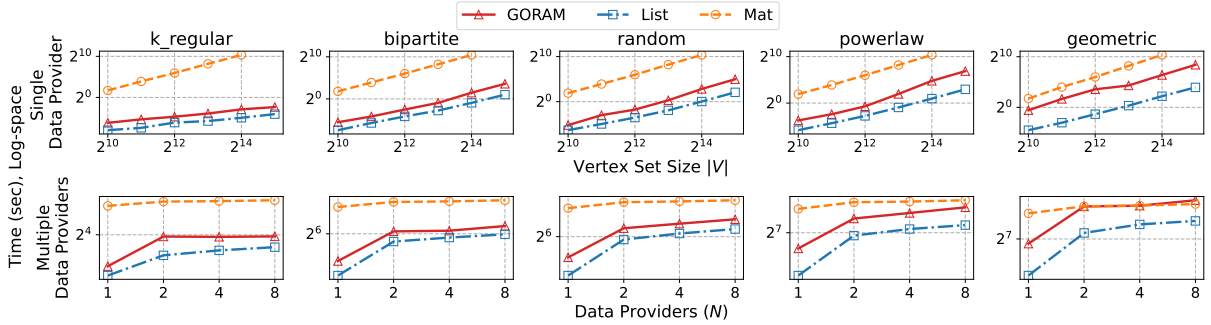


Figure 9: Initialization Cost

random seeds and construct the 2d-partitioned structure to obtain the partition size l as Section 4 illustrates without padding. As Figure 7 shows, the range of l is relatively narrow for all distributions. E.g., l varies within a range of 188 in k_{regular} and only varies within a range of 11 in random graph. Notably, the partition size l is significantly smaller than $|E|$ for all five graph types (see Table 3), suggesting that GORAM often significantly outperforms *List*.

Query execution time. Each row of Figure 8 presents the execution time of a query across different graph densities from the sparsest to the densest, using both GORAM and the two strawman solutions. Overall, we observe that GORAM delivers highly efficient query responses across all 90 test cases (6 sizes \times 5 graph distributions \times 3 queries), offering an average query completion time of 22.0 ms. We provide a detailed performance analysis below.

Performance vs. graph density and size. *Mat* is the least sensitive to graph density (e.g., all around 2^6 ms across the first row), because its query processing time only depends on $|V|$ (see Table 1). *List*, on the contrary, is very sensitive to density, given its $O(|E|)$ processing time per query. GORAM, on the other hand, works well across different densities, exhibiting sub-linear execution time on both $|V|$ and the graph density. The trend in execution time precisely matches the theoretical complexities in Table 1.

For sparse graphs (first two columns in Figure 8), *Mat* performs the worst on almost all $|V|$ settings, as expected, because it spends too much resource processing empty cells. *List* performs as well as, or even better than GORAM on very small graphs (i.e., 1024 vertices) for *NeighborsGet*. This is because *NeighborsGet* requires multiple secure comparison and multiplication operations, and the communication round latency becomes the bottleneck for small graphs. *List*, in this case, saves the communication rounds required for partition access, providing advantages compared to GORAM. However, the performance gets worse fast as $|V|$ increases, because the $O(|E|)$ complexity of *List* quickly dominates the performance.

For dense graphs (last two columns in Figure 8), *Mat* gets closer performance with GORAM as far as it supports the scale, but *List* performs poorly except for the smallest cases. In fact, in the largest version of the densest geometric graph, *List* can be as much as $703.6\times$ slower because of its $O(|E|)$ complexity.

Performance with queries. *Mat* is always several times slower than GORAM on *NeighborsGet*, because it takes $O(\log(|V|))$ time to access the adj-VORAM while GORAM only takes $O(\log(b))$, $b = \frac{|V|}{k}$.

For *EdgeExist*, although GORAM still requires less ORAM access time, the advantage is less significant because it introduces $O(\log(l))$ communication rounds of OR to aggregate the partition

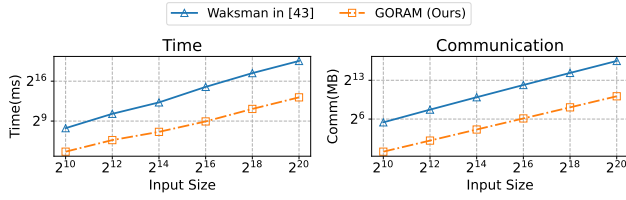


Figure 10: ShuffleMem Construction (* the y-axes are in log-scale.)

(see Section 5.1). However, *Mat* only needs a single round of comparison to process a single cell. Therefore, *Mat* becomes closer to GORAM for denser graphs with larger l .

The slowest query of GORAM is the NeighborsGet on the largest geometric graph, which takes 132.8 ms. The performance of GORAM and *Mat* are very close except for the sparsest k -regular. This is because GORAM requires multiple expensive secure operations on the vertex partition with bl edges while *Mat* only needs a single comparison on $|V|$ matrix cells, which becomes faster than GORAM for denser graphs, offsets the higher overhead of ORAM access, i.e., $O(\log(|V|))$ for *Mat* while $O(\log(b))$ for GORAM.

Initialization performance. The first row in Figure 9 shows the initialization cost when there is only one data provider. The cost is the wall-clock time from data loading to secure indices construction (affecting only GORAM and *Mat*, as *List* does not require establishing indices). The initialization cost is linear to the graph sizes, i.e., $|V|^2$ or $|E|$. Given the relationship $|E| < b^2l < |V|^2$ among *List*, GORAM, and *Mat*, the initialization costs follow the order: *Mat* > GORAM > *List*, as shown in Figure 9. *Mat* has the highest and constant cost across sparse and dense graphs because of its $O(|V|^2)$ complexity. Notably, *Mat* runs out of memory during the construction of adj-ORAM on all graphs with 32K vertices, even with 512GB memory.

Initialization performance with multiple data providers. The second row in Figure 9 presents the cost when there are multiple data providers (1 to 8). We simulate the distributed graphs by randomly assigning each edge of the synthetic graph with 16K vertices to each data provider, which is the largest scale *Mat* supports. For $N > 1$ data providers, both GORAM and *List* need to perform the merge sort on N^+ or N ordered private graphs (see Section 4.2), which leads to more overhead. However, the impact of an increase in N is not significant as Figure 9 shows. This is because the introduced workload is logarithmic, i.e., $\log(N)$ or $\log(N^+)$, $N^+ \approx \frac{l}{l'}$.

ShuffleMem construction comparison. Figure 10 compares the cost of ShuffleMem construction of an array of n secret-shared integers using *Waksman* permutation network, as adopted in [66], and our optimized constant-round ShuffleMem protocol introduced in Section 4.4. The ShuffleMem construction is the main bottleneck of building ORAM. We can see that GORAM significantly accelerates both computation and communication, achieving 17.4× to 83.5× speedups and 97.5% to 98.8% communication savings as input sizes increase. This is because our method reduces the original $O(n \log(n))$ computation and communication to $O(n)$, thereby showing better performance as input sizes increase. Furthermore, unlike *Waksman* network, which necessitates an expensive switch operation, amounting to approximately $\approx 6n$ communications per layer in the $2 \log(n)$ depth network, GORAM only requires shares transmission and XOR operations that do not need communications.

8 Related Work

We discuss the prior arts related to GORAM.

Secure federated databases focus on conducting *public* SQL queries over federated databases while protecting the individual tuples. Examples include [13–15, 33, 39, 58]. For each query, these databases analyze the statements and run secure protocols on the required data to obtain the result. Based on the above progress, Aljuaid et al. [8, 9] propose to process federated graph queries by directly translating the graph queries into SQL through [35]. Compared with these *public* query systems, we focus on ego-centric queries with private query keys.

Secure graph processing with theoretical guarantees. Beyond the *Mat* and *List* introduced in Section 3.2, there are proposals leveraging *Structured Encryption* (SE) [25] to query graphs securely. They focus on encrypting the graph in a way that can be privately queried [30, 38, 48, 61]. However, they require a shared key between the data provider and the client, and consequently, cannot be directly extended to allow multiple data providers and third-party clients. Other studies [42, 55] focus on private analytics over a set of devices organized as a graph, a topic orthogonal to our work.

Graph processing under other security settings. Numerous proposals focus on conducting graph queries guaranteeing *differential privacy* (DP) on two neighboring graphs, e.g., graphs differ on one vertex or edge, like [34, 36, 42, 46, 47, 54, 59, 60]. They focus on protecting inputs from the results. In addition to the unavoidably inaccurate results, they pay less attention to the information leakage during the computation. E.g., FEAT [42] leaks noisy vertex degrees, which may be close approximations to control errors. GORAM, however, focuses on protecting *all* the information during the computation except the result, which is orthogonal to DP’s goal. There are proposals leveraging TEEs [22–24, 62], which are vulnerable to side-channel attacks [43, 50].

DORAM implementations. FLORAM [29] and DuORAM [57] focus on high-latency and low-bandwidth settings. They trade a linear computation complexity for reduced communications, therefore becoming impractical for large-scale data. 3PC-DORAM [20], GigaORAM [29], and Square-root ORAM [66] struggle for sub-linear complexity. GigaORAM and 3PC-DORAM depend on the *Shared-In Shared-Out Pseudo Random Functions* (SISO-PRF) to improve complexity. However, the SISO-PRF becomes practical only with “MPC friendly” block ciphers, i.e., LowMC [7], which was unfortunately cryptanalyzed [40]. GORAM builds its indices on Square-root ORAM, ensuring sublinear complexity and robust security guarantee.

9 Conclusion and Future Work

We propose GORAM, the first step towards achieving efficient private ego-centric queries on federated graphs. GORAM introduces a methodology for reducing the to-be-processed data sizes in secure computations, relying on query-specific data partitioning and secure indices. We hope this method can be generalized to other applications beyond ego-centric queries. Extensive evaluations validate that GORAM achieves practical performance on real-world graphs, even with 1.4 billion edges. For future work, we aim to expand GORAM’s capabilities for more advanced applications, including complex graph queries like path filtering and pattern matching, while also optimizing its performance and scalability.

References

- [1] 2006. https://igraph.org/python/api/0.9.11/igraph._igraph.GraphBase.html#K-Regular
- [2] 2006. <https://igraph.org/python/api/0.9.11/igraph.Graph.html#Random-Bipartite>
- [3] 2006. https://igraph.org/python/api/0.9.11/igraph._igraph.GraphBase.html#Erdos_Renyi
- [4] 2006. https://igraph.org/python/api/0.9.11/igraph._igraph.GraphBase.html#Barabasi
- [5] 2006. https://igraph.org/python/api/0.9.11/igraph._igraph.GraphBase.html#_GRG
- [6] 2009. Community Structure in Large Networks: Natural Cluster Sizes and the Absence of Large Well-Defined Clusters. In *Internet Mathematics*.
- [7] Martin R Albrecht, Christian Rechberger, Thomas Schneider, Tyge Tiessen, and Michael Zohner. 2015. Ciphers for MPC and FHE. In *Advances in Annual International Conference on the Theory and Applications of Cryptographic Techniques (EUROCRYPT)*.
- [8] Nouf Aljuaid, Alexei Lisitsa, and Sven Schewe. 2023. Secure Joint Querying Over Federated Graph Databases Utilizing SMPC Protocols. In *ICISSP*.
- [9] Nouf Aljuaid, Alexei Lisitsa, and Sven Schewe. 2024. Efficient and Secure Multi-party Querying over Federated Graph Databases. In *International Conference on Data Science, Technology and Applications (DATA)*.
- [10] Toshinori Araki, Jun Furukawa, Kazuma Ohara, Benny Pinkas, Hanan Rosemarin, and Hikaru Tsuchida. 2021. Secure Graph Analysis at Scale. In *Proceedings of the ACM SIGSAC Conference on Computer and Communications Security (CCS)*.
- [11] Timothy G Armstrong, Vamsi Ponnkanti, Dhruva Borthakur, and Mark Callaghan. 2013. LinkBench: a Database Benchmark based on the Facebook Social Graph. In *Proceedings of the International Conference on Management of Data (SIGMOD)*.
- [12] Gilad Asharov, Koki Hamada, Ryo Kikuchi, Ariel Nof, Benny Pinkas, and Junichi Tomida. 2023. Secure Statistical Analysis on Multiple Datasets: Join and Group-By. In *Proceedings of the ACM SIGSAC Conference on Computer and Communications Security (CCS)*.
- [13] Johes Bater, Gregory Elliott, Craig Eggen, Satyender Goel, Abel N Kho, and Jennie Rogers. 2017. SMCQL: Secure Query Processing for Private Data Networks. In *Proceedings of the VLDB Endowment*.
- [14] Johes Bater, Xi He, William Ehrlich, Ashwin Machanavajhala, and Jennie Rogers. 2018. Shrinkwrap: efficient SQL query processing in differentially private data federations. In *Proceedings of the VLDB Endowment*.
- [15] Johes Bater, Yongjoo Park, Xi He, Xiao Wang, and Jennie Rogers. 2020. SAQE: Practical Privacy-preserving Approximate Query Processing for Data Federations. In *Proceedings of the VLDB Endowment*.
- [16] Marina Blanton, Aaron Steele, and Mehrdad Alisagari. 2013. Data-oblivious Graph Algorithms for Secure Computation and Outsourcing. In *Proceedings of the ACM Asia Conference on Computer and Communications Security (ASIA-CCS)*.
- [17] Dan Bogdanov, Sven Laur, and Jan Willemson. 2008. Sharemind: A Framework for Fast Privacy-preserving Computations. In *European Symposium on Research in Computer Security (ESORICS)*. Springer.
- [18] Paolo Boldi and Sebastiano Vigna. 2004. The Webgraph Framework I: Compression Techniques. In *Proceedings of the International Conference on World Wide Web (WWW)*.
- [19] Nathan Bronson, Zach Amsden, George Cabrera, Prasad Chakka, Peter Dimov, Hui Ding, Jack Ferris, Anthony Giardullo, Sachin Kulkarni, Harry Li, et al. 2013. TAO: Facebook's Distributed Data Store for The Social Graph. In *USENIX Annual Technical Conference (ATC)*.
- [20] Paul Bunn, Jonathan Katz, Eyal Kushilevitz, and Rafail Ostrovsky. 2020. Efficient 3-party Distributed ORAM. In *Security and Cryptography for Networks (SCN)*.
- [21] Ran Canetti. 2000. Security and Composition of Multiparty Cryptographic Protocols. In *Journal of CRYPTOLOGY*.
- [22] Javad Ghareh Chamani, Ioannis Demertzis, Dimitrios Papadopoulos, Charalampos Papamanthou, and Rasool Jalili. 2024. GraphOS: Towards Oblivious Graph Processing. In *Proceedings of the VLDB Endowment*.
- [23] Zhao Chang, Dong Xie, Sheng Wang, and Feifei Li. 2022. Towards Practical Oblivious Join. In *Proceedings of the International Conference on Management of Data (SIGMOD)*.
- [24] Zhao Chang, Lei Zou, and Feifei Li. 2016. Privacy Preserving Subgraph Matching on Large Graphs in Cloud. In *Proceedings of the International Conference on Management of Data (SIGMOD)*.
- [25] Melissa Chase and Seny Kamara. 2010. Structured Encryption and Controlled Disclosure. In *International Conference on the Theory and Application of Cryptology and Information Security (ASIACRYPT)*.
- [26] Fan Chung. 2010. Graph Theory in the Information Age. In *Notices of the AMS*.
- [27] Daniel Demmler, Thomas Schneider, and Michael Zohner. 2015. ABY-A framework for Efficient Mixed-protocol Secure Two-party Computation. In *The Network and Distributed System Security Symposium (NDSS)*.
- [28] Jack Doerner and Abhi Shelat. 2017. Scaling ORAM for Secure Computation. In *Proceedings of the ACM SIGSAC Conference on Computer and Communications Security (CCS)*.
- [29] Brett Falk, Rafail Ostrovsky, Matan Shtepel, and Jacob Zhang. 2023. GigaDORAM: breaking the billion address barrier. In *Proceedings of the USENIX Conference on Security Symposium (USENIX Security)*.
- [30] Francesca Falzon, Esha Ghosh, Kenneth G Paterson, and Roberto Tamassia. 2024. PathGES: An Efficient and Secure Graph Encryption Scheme for Shortest Path Queries. In *Proceedings of the ACM SIGSAC Conference on Computer and Communications Security (CCS)*.
- [31] Oded Goldreich and Rafail Ostrovsky. 1996. Software Protection and Simulation on Oblivious RAMs. In *Journal of the ACM (JACM)*.
- [32] Tamás Nepusz Gábor Csárdi. 2006. The igraph Software Package for Complex Network Research. In *InterJournal Complex Systems*.
- [33] Feng Han, Lan Zhang, Hanwen Feng, Weiran Liu, and Xiangyang Li. 2022. Scape: Scalable collaborative analytics system on private database with malicious security. In *IEEE International Conference on Data Engineering (ICDE)*.
- [34] Jacob Imola, Takao Murakami, and Kamalika Chaudhuri. 2021. Locally Differentially Private Analysis of Graph Statistics. In *Proceedings of the USENIX Conference on Security Symposium (USENIX Security)*.
- [35] Alekh Jindal, Prayna Rawlani, Eugene Wu, Samuel Madden, Amol Deshpande, and Mike Stonebraker. 2014. Vertexica: Your Relational Friend for Graph Analytics!. In *Proceedings of the VLDB Endowment*.
- [36] Vishesh Karwa, Sofya Raskhodnikova, Adam Smith, and Grigory Yaroslavtsev. 2011. Private Analysis of Graph Structure. In *Proceedings of the VLDB Endowment*.
- [37] Nishat Koti, Varsha Bhat Kukkal, Arpita Patra, and Bhavish Raj Gopal. 2024. Graphiti: Secure Graph Computation Made More Scalable. In *ACM SIGSAC Conference on Computer and Communications Security (CCS)*.
- [38] Shangqi Lai, Xingliang Yuan, Shi-Feng Sun, Joseph K Liu, Yuhong Liu, and Dongxi Liu. 2019. GraphSE²: An Encrypted Graph Database for Privacy-preserving Social Search. In *Proceedings of the ACM Asia Conference on Computer and Communications Security (ASIA-CCS)*.
- [39] John Liagouris, Vasiliki Kalavri, Muhammad Faisal, and Mayank Varia. 2023. SECURECY: Secure Collaborative Analytics in Untrusted Clouds. In *USENIX Symposium on Networked Systems Design and Implementation (NSDI)*.
- [40] Fukang Liu, Takanori Isobe, and Willi Meier. 2021. Cryptanalysis of Full LowMC and LowMC-M with Algebraic Techniques. In *Advances in Annual International Cryptology Conference (CRYPTO)*.
- [41] Kunlong Liu and Trinabh Gupta. 2024. Making Privacy-preserving Federated Graph Analytics with Strong Guarantees Practical (for Certain Queries). In *Proceedings of the 29th ACM Symposium on Access Control Models and Technologies (SACMAT)*.
- [42] Shang Liu, Yang Cao, Takao Murakami, Weiran Liu, Seng Pei Liew, Tsubasa Takahashi, Jinfei Liu, and Masatoshi Yoshikawa. 2023. Federated Graph Analytics with Differential Privacy. In *International Workshop on Federated Learning for Distributed Data Mining*.
- [43] Xiaoxuan Lou, Tianwei Zhang, Jun Jiang, and Yinqian Zhang. 2021. A Survey of Microarchitectural Side-channel Vulnerabilities, Attacks, and Defenses in Cryptography. In *ACM Computing Surveys (CSUR)*.
- [44] Steve Lu and Rafail Ostrovsky. 2013. Distributed Oblivious RAM for Secure Two-party Computation. In *Theory of Cryptography Conference (TCC)*.
- [45] Nav Mathur. 2021. Graph Technology for Financial Services. Neo4j. <https://go.neo4j.com/rs/710-RRC-335/images/Neo4j-in-Financial%20Services-white-paper.pdf> (White Paper).
- [46] Sahar Mazloom and S Dov Gordon. 2018. Secure Computation with Differentially Private Access Patterns. In *Proceedings of the ACM SIGSAC Conference on Computer and Communications Security (CCS)*.
- [47] Sahar Mazloom, Phi Hung Le, Samuel Ranellucci, and S Dov Gordon. 2020. Secure Parallel Computation on National Scale Volumes of Data. In *Proceedings of the USENIX Conference on Security Symposium (USENIX Security)*.
- [48] Xianrui Meng, Seny Kamara, Kobbi Nissim, and George Kollios. 2015. GRECS: Graph Encryption for Approximate Shortest Distance Queries. In *Proceedings of the ACM SIGSAC Conference on Computer and Communications Security (CCS)*.
- [49] Payman Mohassel and Peter Rindal. 2018. ABY3: A Mixed Protocol Framework for Machine Learning. In *ACM SIGSAC conference on computer and communications security (CCS)*.
- [50] Antonio Muñoz, Ruben Rios, Rodrigo Román, and Javier López. 2023. A survey on the (in) security of trusted execution environments. In *Computers & Security*. Elsevier.
- [51] Kartik Nayak, Xiao Shaun Wang, Stratis Ioannidis, Udi Weinsberg, Nina Taft, and Elaine Shi. 2015. GraphSC: Parallel Secure Computation Made Easy. In *IEEE Symposium on Security and Privacy (S&P)*.
- [52] Shen Noether, Adam Mackenzie, et al. 2016. Ring confidential transactions. *Ledger* (2016).
- [53] Xiafei Qiu, Wubin Cen, Zhengping Qian, You Peng, Ying Zhang, Xuemin Lin, and Jingren Zhou. 2018. Real-time Constrained Cycle Detection in Large Dynamic Graphs. In *Proceedings of the VLDB Endowment*.

- [54] Leyla Roohi, Benjamin IP Rubinstein, and Vanessa Teague. 2019. Differentially-private Two-party Egocentric Betweenness Centrality. In *IEEE INFOCOM Conference on Computer Communications*.
- [55] Edo Roth, Karan Newatia, Yiping Ma, Ke Zhong, Sebastian Angel, and Andreas Haeberlen. 2021. Mycelium: Large-scale distributed graph queries with differential privacy. In *Proceedings of the ACM SIGOPS Symposium on Operating Systems Principles (SOSP)*.
- [56] Emil Stefanov, Marten van Dijk, Elaine Shi, T-H Hubert Chan, Christopher Fletcher, Ling Ren, Xiangyao Yu, and Srinivas Devadas. 2018. Path ORAM: an extremely simple oblivious RAM protocol. In *Journal of the ACM (JACM)*.
- [57] Adithya Vadamalli, Ryan Henry, and Ian Goldberg. 2023. DuORAM: A Bandwidth-Efficient Distributed ORAM for 2-and 3-Party Computation. In *Proceedings of the USENIX Conference on Security Symposium (USENIX Security)*.
- [58] Nikolaj Volgushev, Malte Schwarzkopf, Ben Getchell, Mayank Varia, Andrei Lapets, and Azer Bestavros. 2019. Conclave: Secure Multi-party Computation on Big Data. In *Proceedings of The European Conference on Computer Systems (EuroSys)*.
- [59] Songlei Wang, Yifeng Zheng, and Xiaohua Jia. 2024. GraphGuard: Private Time-Constrained Pattern Detection Over Streaming Graphs in the Cloud. In *USENIX Security Symposium (USENIX Security)*.
- [60] Songlei Wang, Yifeng Zheng, Xiaohua Jia, Qian Wang, and Cong Wang. 2023. MAGO: Maliciously Secure Subgraph Counting on Decentralized Social Graphs. In *IEEE Transactions on Information Forensics and Security (TIFS)*.
- [61] Songlei Wang, Yifeng Zheng, Xiaohua Jia, and Xun Yi. 2022. PeGraph: A System for Privacy-Preserving and Efficient Search Over Encrypted Social Graphs. In *IEEE Transactions on Information Forensics and Security (TIFS)*.
- [62] Lyu Xu, Byron Choi, Yun Peng, Jianliang Xu, and Sourav S Bhowmick. 2023. A framework for privacy preserving localized graph pattern query processing. In *Proceedings of the International Conference on Management of Data (SIGMOD)*.
- [63] Jaewon Yang and Jure Leskovec. 2012. Defining and Evaluating Network Communities Based on Ground-truth. In *Proceedings of the ACM SIGKDD Workshop on Mining Data Semantics*.
- [64] Juncheng Yang, Yao Yue, and KV Rshmi. 2021. A large-scale analysis of hundreds of in-memory key-value cache clusters at twitter. In *ACM Transactions on Storage (TOS)*.
- [65] A. C. Yao. 1986. How to Generate and Exchange Secrets. In *27th Annual Symposium on Foundations of Computer Science (FOCS)*.
- [66] Samee Zahur, Xiao Wang, Mariana Raykova, Adrià Gascón, Jack Doerner, David Evans, and Jonathan Katz. 2016. Revisiting Square-root ORAM: Efficient Random Access in Multi-party Computation. In *IEEE Symposium on Security and Privacy (S&P)*.

A Security Analysis

A.1 Security Proof of ShuffleMem

In this section, we provide a formal proof of Theorem 1, following strictly to the *real-world / ideal-world paradigm* [21]. Let \mathcal{A} denote the real-world adversary, and \mathcal{S} denote the ideal-world adversary. We prove that for *any* semi-honest \mathcal{A} controlling at most one party, there exists a \mathcal{S} running in polynomial of the running time of \mathcal{A} , such that for all inputs and all sets of corrupted parties, the view of \mathcal{S} is indistinguishable from the view of \mathcal{A} (Equation 1).

We prove the security of Protocol 1 in the $\mathcal{F}_{\text{setup}}$ -hybrid world, where there exists an ideal functionality $\mathcal{F}_{\text{setup}}$ that generates common *pseudorandom keys (PRF)* among the computation parties, i.e., each pair of computation servers, S_i and S_j , has a common key s_{ij} to generate correlated randomness, and the key is exclusively known to the pair of computation servers. The security of protocols implemented $\mathcal{F}_{\text{setup}}$ is well-established, and [37] provides the formal proof; therefore, we omit it here for brevity.

In the following, we define the ideal functionality of ShuffleMem, i.e., $\mathcal{F}_{\text{ShuffleMem}}$, and then provide the construction of the simulator \mathcal{S} to prove the security of Protocol 1.

The definition of $\mathcal{F}_{\text{ShuffleMem}}$ is shown in Figure 11, which is defined as a trusted third party that randomly shuffles the secret shared array $D \equiv A \oplus B \oplus C$ using a random permutation π and returns the secret shares of the shuffled array $\tilde{D} = \pi(D)$ and the permutation representation $\tilde{\pi}$ to the corresponding computation

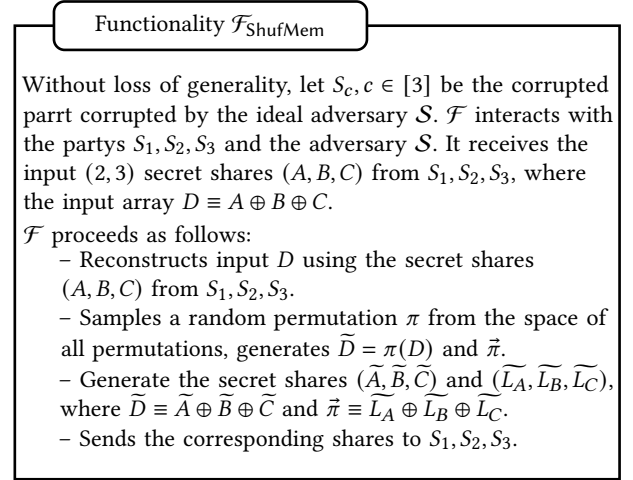


Figure 11: Ideal Functionality $\mathcal{F}_{\text{ShufMem}}$.

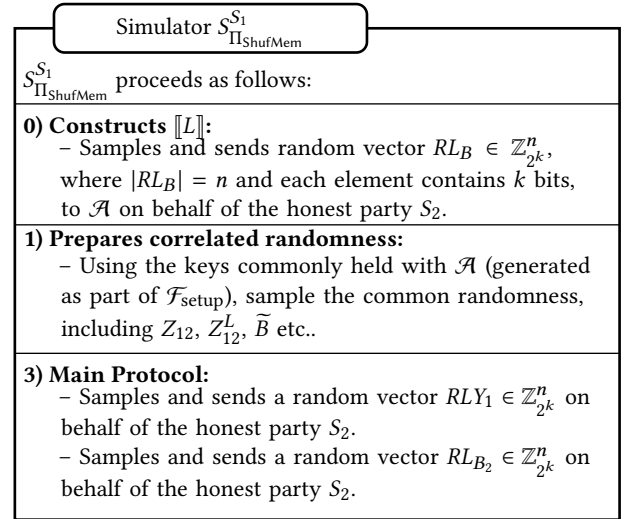


Figure 12: Simulator $\mathcal{S}_{\Pi_{\text{ShufMem}}}^{S_1}$ Construction.

servers. Then, we prove that the real-world protocol $\Pi_{\text{ShuffleMem}}$ (Protocol 1) securely realizes $\mathcal{F}_{\text{ShuffleMem}}$ in the presence of *any* semi-honest adversary \mathcal{A} . Without loss of generality, the simulator is constructed assuming \mathcal{A} corrupts the party S_1 . The simulation for S_2 and S_3 is similar.

PROOF. Let \mathcal{A} denote the real-world adversary corrupting S_1 , and $\mathcal{S}_{\Pi_{\text{ShufMem}}}^{S_1}$ denote the corresponding ideal-world adversary. The construction of $\mathcal{S}_{\Pi_{\text{ShufMem}}}^{S_1}$ is shown in Figure 12.

For the 0) step in Protocol 1, the simulator $\mathcal{S}_{\Pi_{\text{ShufMem}}}^{S_1}$ samples and sends a random vector $RL_B \in \mathbb{Z}_{2^k}^n$ to \mathcal{A} (since \mathcal{A} corrupts S_1) on behalf of the honest party S_2 . Because the real-world message $L_B = Z_2$ is uniformly random in the view of \mathcal{A} , \mathcal{A} cannot distinguish the real-world messages L_B with the randomly sampled message RL_B from the simulator.

For the 1) step, S emulates $\mathcal{F}_{\text{setup}}$ at first, during which S generates the PRFs between the corrupted S_1 and S_2, S_3 , i.e., s_{12}, s_{13} . Then, S generates the correlated randomness held by S_1 , including $Z_{12}, Z_{12}^L, \tilde{B}$ etc..

For the 3) step, S randomly samples RLY_1 and RLB_2 on behalf of S_2 and sends to \mathcal{A} . In the real-world scenario, the values LY_1 and LB_2 received by \mathcal{A} are masked using Z_{23}^L and \tilde{L}_C , which are uniformly random from \mathcal{A} 's viewpoint. Consequently, the messages LY_1 and LB_2 appear uniformly random to \mathcal{A} and are indistinguishable from the messages provided by the simulator.

In summary, the view of \mathcal{A} in the real-world (i.e., interacting with honest servers S_2 and S_3) is indistinguishable from the view of the ideal-world (i.e., interacting with a simulator $S_{\Pi_{\text{ShufMem}}}^{S_1}$). Therefore, we have Theorem 1 holds. \square

B Complexity Analysis

In this section, we analyze the complexities summarized in Table 1.

Initialization. The initialization of *Mat* and *List* are dominated by the adj-VORAM, adj-EORAM constructions, and odd_even_merge_sort networks, respectively. GORAM, however, includes both stages while each stage needs lower-complexity because of the partitioned data structure (see Section 4).

For *Mat*, the initialization includes a linear-complexity ShuffleMem and a logmatrix-complexity position map construction. Since *Mat* requires a $|V|^2$ adjacency matrix each data provider, the computation complexity is $O(N|V|^2)$. The communication rounds include the 3 rounds for the ShuffleMem Protocol 1 (Section 4.4) and $2 \log_P(\frac{|V|}{T})$ or $2 \log_P(\frac{|V|^2}{T})$ rounds for the position map construction of adj-VORAM and adj-EORAM, respectively (Section 4.1).

For *List*, the initialization complexity is the complexity of the odd_even_merge_sort network for N data providers. Because the complexity of the merge sort network is $O(n \log(n))$ and the communication rounds is the $O(\log(n))$, the complexity of sorting of N lists with $|E|$ elements is $O(|E| \log(|E|) \log(N))$, and the communication rounds is $O(\log(|E|) \log(N))$.

For GORAM, the initialization contains both ORAM initialization over the partitions and odd_even_merge_sort for each partition. Since each of the b^2 partitions can be processed in parallel, the merging round complexity is $\log(l) \log(N^+)$, where l is the partition size and N^+ is the number of all the submitted partitioned graphs. Therefore, the complexity to initialize GORAM is $O(b^2 l \log(l) \log(N^+))$, where the b^2 sorting network is the main bottleneck. The communication rounds include 3 for the ShuffleMem Protocol 1, $O(\log(l) \log(N^+))$ for the sorting network, and $2 \log_P(\frac{b}{T})$ or $2 \log_P(\frac{b^2}{T})$ for the position map construction of VO-RAM and EORAM, respectively.

Partition Access. For *Mat* and GORAM that utilize ORAM, the partition access complexity is the same as the ORAM access complexity. By substituting the n term in the ORAM access complexity, i.e., $O(PT \log_P(\frac{n}{T}))$, we have that the partition access complexity for *Mat* is $O(PT \log_P(\frac{|V|^2}{T}))$ and $O(PT \log_P(\frac{|V|}{T}))$ for adj-EORAM

Algorithm 4: GetPosBase

Inputs : ORAM in the last level containing T blocks, $\llbracket i \rrbracket$ denote the secret index in this level, $\llbracket \text{fake} \rrbracket$.

Output : Physical index p .

```

// For  $\llbracket s_2 \rrbracket$  without  $\llbracket \text{fake} \rrbracket$  in [66]
1  $\llbracket \text{notUsed} \rrbracket \leftarrow \text{ORAM}.\llbracket \text{Used} \rrbracket$ ;
2  $\llbracket \text{fZero} \rrbracket \leftarrow \llbracket 0, \text{notUsed}_0, \text{notUsed}_1, \dots, \text{notUsed}_{T-2} \rrbracket$ ;
3 for  $i \leftarrow 0$  to  $\lfloor \log_2(T) \rfloor$  do
4    $s = 2^i$  denoting the stride;
5    $\llbracket \text{fZero} \rrbracket_{s:T} \leftarrow \text{OR}(\llbracket \text{fZero} \rrbracket_{s:T}, \llbracket \text{fZero} \rrbracket_{0:T-s})$ ;
6 end
7  $\llbracket \text{fZero} \rrbracket.\text{append}(\llbracket 1 \rrbracket)$ ;
8  $\llbracket \text{fZero} \rrbracket_{0:T} \leftarrow \text{XOR}(\llbracket \text{fZero} \rrbracket_{0:T}, \llbracket \text{fZero} \rrbracket_{1:T+1})$ ;
// Update  $\llbracket \text{Used} \rrbracket$ 
// For  $\llbracket s_1 \rrbracket$  without  $\llbracket \text{fake} \rrbracket$  in [66]
9  $\llbracket s_1 \rrbracket \leftarrow \text{EQ}(\text{expanded}(\llbracket i \rrbracket), [0, 1, \dots, T-1])$ ;
// Considering  $\llbracket \text{fake} \rrbracket$ 
10  $\llbracket \text{mask} \rrbracket \leftarrow \llbracket s_1 \rrbracket$  if  $\llbracket \text{fake} \rrbracket$  else  $\llbracket \text{fZero} \rrbracket$  obviously;
// Update  $\llbracket \text{Used} \rrbracket$ 
11  $\text{ORAM}.\llbracket \text{Used} \rrbracket = \text{OR}(\llbracket \text{mask} \rrbracket, \text{ORAM}.\llbracket \text{Used} \rrbracket)$ ;
// Get the corresponding index
12  $\llbracket \text{index} \rrbracket \leftarrow \text{DOT}(\text{ORAM}.\llbracket \text{Data} \rrbracket, \llbracket \text{mask} \rrbracket)$ ;
13 Reveal  $p \leftarrow$  index in plaintext;
14 return  $p$ ;
```

and adj-VORAM, respectively. Similarly, the partition access complexity for GORAM is $O(PT \log_P(\frac{b^2}{T}))$ and $O(PT \log_P(\frac{b}{T}))$ because there are b^2 and b partitions in the EORAM and VORAM, respectively.

The *List*, however, does not contain ORAM, and the partition access complexity is $O(1)$, i.e., directly access the whole list.

Partition Processing for Basic Queries. The complexities of the partition processing are basically the complexity of scanning the whole partition.

For the edge-centric query, EdgeExist, the partition size of *Mat*, *List* and GORAM is 1 (i.e., a single element in the adjacency matrix), $|E|$ and l (i.e., a single partition); therefore, the complexity of this query is $O(1)$, $O(|E|)$ and $O(l)$, respectively. Because the aggregation operation OR requires communication, therefore the round complexity is $O(1)$, $O(\log(N))$ and $O(\log(l))$ for *Mat*, *List* and GORAM, respectively.

For the vertex-centric queries, i.e., NeighborsCount and NeighborsGet, the partition size of *Mat*, *List* and GORAM is $|V|$ (i.e., a single row in the adjacency matrix), $|E|$ and bl ; therefore, the complexity of these queries is $O(|V|)$, $O(|E|)$ and $O(bl)$, respectively. Because the aggregation operation in NeighborsCount is communication-free ADD and NeighborsGet does not need aggregation, the round complexity for all three data structures across the two queries is $O(1)$.

C Prefix-based ORAM.Access

The original Square-root ORAM [66] uses a $O(n)$ rounds method in the last level of its recursive ORAM (GetPosBase function, in Section D, Figure 6), and in GORAM, we optimize it to $O(\log(n))$ rounds. The interfaces and the methods are shown in Algorithm 4, keeping the same notations as the original Square-root ORAM.

Algorithm 5: UniqueNeighborsCount

Inputs : Target vertex $\llbracket v \rrbracket$ and the target block ID $\llbracket i \rrbracket = \lceil \frac{v}{K} \rceil$.
Output: $\llbracket \text{num} \rrbracket^A$, the number of v 's unique outing neighbors.
// Sub-graph extraction.
1 Fetch the target edge blocks $\llbracket B \rrbracket \leftarrow \text{VORAM.access}(\llbracket i \rrbracket)$, where $\llbracket B \rrbracket$ contains **(bl)** source_nodes and dest_nodes;
// Parallely sub-graph process.
// 1) Mask-out the non-neighbors.
2 Construct $\llbracket \vec{v} \rrbracket$ by expanding $\llbracket v \rrbracket$ bl times;
3 Compute $\llbracket \text{mask} \rrbracket \leftarrow \text{EQ}(\llbracket \vec{v} \rrbracket, \llbracket B \rrbracket.\text{source_nodes})$;
4 Compute $\llbracket \text{candidate} \rrbracket \leftarrow \text{MUL}(\llbracket \text{mask} \rrbracket, \llbracket B \rrbracket.\text{dest_nodes})$;
// 2) De-duplicate neighbors.
5 $\llbracket \text{same_mask} \rrbracket \leftarrow \text{EQ}(\llbracket \text{candidate} \rrbracket_{[1:]}, \llbracket \text{candidate} \rrbracket_{[:-1]})$;
6 $\llbracket \text{same_mask} \rrbracket.\text{append}(\llbracket 1 \rrbracket)$;
7 $\llbracket \text{mask} \rrbracket \leftarrow \text{MUL}(\llbracket \text{same_mask} \rrbracket, \llbracket \text{mask} \rrbracket)$;
// 3) Aggregating for the final outcomes.
8 Compute $\llbracket \text{mask} \rrbracket^A \leftarrow \text{B2A}(\llbracket \text{mask} \rrbracket)$;
9 **while** $\lceil \frac{l}{2} \rceil \geq 1$ **do**
10 Pads $\llbracket 0 \rrbracket^A$ to $\llbracket \text{mask} \rrbracket^A$ to be even ;
11 Split $\llbracket \text{mask} \rrbracket^A$ half-by-half to $\llbracket \text{mask} \rrbracket_l^A$ and $\llbracket \text{mask} \rrbracket_r^A$;
12 Aggregate $\llbracket \text{mask} \rrbracket^A \leftarrow \text{ADD}(\llbracket \text{mask} \rrbracket_l^A, \llbracket \text{mask} \rrbracket_r^A)$;
13 $l = \text{len}(\llbracket \text{mask} \rrbracket^A)/2$;
14 **end**
15 $\llbracket \text{num} \rrbracket^A = \llbracket \text{mask} \rrbracket^A$;
16 **return** $\llbracket \text{num} \rrbracket^A$;

The complicated part in Square-root ORAM is the extraction of the first unused element in the last level ORAM obviously as the

used elements are defined by users access patterns. Algorithm 4 locates this information by constructing $\llbracket \text{fZero} \rrbracket$ (first unused element) leveraging the prefix-computations (Lines 1-6), propagating *whether there exist 1 in $\llbracket \text{notUsed} \rrbracket$ before my location, including my location* to the following elements obviously. After line 6, $\llbracket \text{fZero} \rrbracket$ contains a successive $\llbracket 0 \rrbracket$ and follows with $\llbracket 1 \rrbracket$, and the last $\llbracket 1 \rrbracket$ indicates the element which is the first unused element, i.e., the first zero in $\llbracket \text{Used} \rrbracket$, the first one in $\llbracket \text{notUsed} \rrbracket$. Then, we obviously transfers the previous $\llbracket 1 \rrbracket$ to $\llbracket 0 \rrbracket$ by a differential XOR (Lines 7-8). Note that $\llbracket \text{fZero} \rrbracket$ corresponds to the $\llbracket s_2 \rrbracket$ while not considering $\llbracket \text{fake} \rrbracket$ in the original Square-root ORAM.

Lines 9 corresponds to $\llbracket s_1 \rrbracket$ of Square-root ORAM, indicating which element corresponding to the cipher index $\llbracket i \rrbracket$. Note that before Line 10, there are only $\llbracket 1 \rrbracket$ in $\llbracket \text{fZero} \rrbracket$ and $\llbracket s_1 \rrbracket$ and the $\llbracket 1 \rrbracket$ indicates the expected element for $\llbracket \text{fake} \rrbracket$ is false or true use cases. We obviously select $\llbracket \text{fZero} \rrbracket$ or $\llbracket s_1 \rrbracket$ based on $\llbracket \text{fake} \rrbracket$ and obtain the $\llbracket \text{mask} \rrbracket$. Note that the $\llbracket 1 \rrbracket$ in $\llbracket \text{mask} \rrbracket$ indicates the to-be-use elements location, therefore we update $\text{ORAM}.\llbracket \text{Used} \rrbracket$ afterwards (Line 11). Then, we get the corresponding element in $\text{ORAM}.\llbracket \text{Data} \rrbracket$ using dot-product, i.e., only the elements corresponding to $\llbracket 1 \rrbracket$ of $\llbracket \text{mask} \rrbracket$ is preserved, which is the expected physical index.

D Other Queries

We present the implementation of UniqueNeighborsCount in Algorithm 5, which adds a de-duplication phase between the sub-graph extraction and aggregation phases, updating the $\llbracket \text{mask} \rrbracket$ eliminating the duplicate neighbors (Lines 2-7). Specifically, the de-duplication procedure is similar to NeighborsGet without extracting the real neighbors.